A DISTRIBUTION FUNCTION APPROACH TO SIGNAL SHAPE DISCRIMINATION

By

NARENDRA KUMAR GARG

A THESIS

IN

THE FACULTY

OF

ENGINEERING AND COMPUTER SCIENCE

Presented in Partial Fulfillment of
The Requirements for the Degree of
Master of Engineering at
Concordia University
Montreal, Canada

December 1982

ABSTRACT

A DISTRIBUTION FUNCTION APPROACH TO SIGNAL SHAPE DISCRIMINATION

NARENDRA KUMAR GARG

An algorithm based on the properties of the distribution function has been developed for signal detection and classification. Capability of this algorithm, known as the DF algorithm, to detect very small differences in the shape of two signals is shown. It is illustrated that a pure, single peak signal can be distinguished from a similar looking impure, strongly overlapped double peak signal in the presence of measurement noise. Also, the algorithm is applied in the measurement of the distance between two closely spaced point targets in a radar system. The DF algorithm has less normalized r.m.s. error in measuring the normalized distance between two targets, than the error obtained by the conventional threshold and moment algorithms. The percentage improvement in the performance achieved by the DF algorithm over the other algorithms is computed and is seen to be considerably higher for all ranges of target distance and input signal-to-noise ratio.

To the memory of my father.

ACKNOWLEDGEMENTS

The author wishes to express his gratitude to Professor S.D. Morgera for suggesting the problem and for his guidance and assistance during the entire preparation of this thesis.

Thanks are also due to Madeleine Klein for typing the thesis.

This work was supported by the National Science and Engineering Research Council of Canada under Grant (040-187), awarded to Professor S.D. Morgera.

TABLE OF CONTENTS

Page

LIST OF IMPORTANT ABBREVIATIONS AND SYMBOLS

dB	Decibels
$H_N(s)$	Normalized transfer function of Analog filter
$h_A(t)$	Impulse response of Analog filter
Im[ ]	Imaginary part of
L-1	Inverse Laplace transform
p.d.f.	Probability density function
r.m.s.	Root mean square
RCS	Radar Cross section
Re[ ]	Real part of
S/N	Signal to noise
ω_s	Sampling angular frequency
ω_c	Cut off frequency of digital filter
Z	Z-transform
α	Proportionality factor
θ_1, θ_2	Mean values of Gaussian distribution
σ_1, σ_2	Standard deviation of Gaussian distribution
γ	Radio frequency phase difference
τ	Normalized distance (delay)
ε	Normalized r.m.s. error
σ_p	Half pulse width
$\beta_2{}^P{}_{rms}$	RMS value of β_2 for pure measurement signal
$\beta_2{}^N{}_{rms}$	RMS value of β_2 for noisy measurement signal

CHAPTER 1

THE PROBLEM OF SIGNAL SHAPE DISCRIMINATION

1.1 Introduction

The impetus for this work comes from the field of chromatography [1], in which it is necessary to detect a very small difference between the shapes of two signals. In the field of chromatography, if two substances to be examined are different, one being a pure substance and the other a compound substance, the chromatograph or spectra representing them are different and distinguishable from each other. But in certain cases, the compound substance may be a mixture of a pure substance and a very small amount of another pure substance. Then the chromatographic peak of this compound may look quite similar to the peak corresponding to the pure substance. It then becomes difficult to decide whether the given peak is a simple (pure substance) or a composite peak (impure substance). Such a signal classification problem has been solved in Chapter 2 using a technique called the Distribution Function (DF) algorithm.

Two measurement signals, one pure and the other composite (combination of two pure signals) are prepared. The presence of measurement noise is assumed. A reference signal is also prepared in the form of a pure signal. Signals are assumed to be of Gaussian shape. This assumption is suitable for many applications of interest. The distribution function of each

measurement signal is calculated and compared with that of the reference signal. The invariance property of distribution functions is used in defining the invariance in the shape of the signals. A function, ϕ, is obtained in the form of a curve, each time the above comparison is made. Then the method of least squares is used to determine the degree of nonlinearity of the ϕ curve. Finally this estimate of nonlinearity is used in making the decision regarding the similarity of the shapes. To our knowledge, such an approach has not previously been applied to problems of signal classification in the engineering field.

The usefulness and the success of the DF algorithm encouraged the study of a multi-target radar problem. We apply this algorithm to measure the distance in space between two closely spaced point targets. The accurate measurement of the distance between two closely spaced point targets in the presence of noise has been a long standing problem for radar measuring systems.

In radar systems, a pulse of known shape and the amplitude depending upon the radar cross section (RCS) of the target, is received from each point target. As the two point targets are spaced by a certain distance, a phase difference is produced between both the returned pulses. In the receiver these two pulses are added vectorially and a combined two target response is produced. Here again the

pulses are assumed to be of Gaussian shape which, considering the narrow beam antennas, is a most realistic assumption. The application of the DF algorithm for measuring the distance between two point targets is described in Chapter 3 of this work. The rms value of the error made in the measurement of the distance is calculated in order to judge the performance of the DF algorithm. Equal RCS of the targets is assumed in this application. The performance of the DF algorithm is compared with other existing algorithms in terms of normalized rms error made by each algorithm.

The idea behind this work and the applications as described in Chapter 2 and 3, can be understood more clearly and appreciated with the help of Figure 1.1.

1.2 Main Features of the DF Algorithm

The main feature of this algorithm is that it uses the normalized integrals of the signals to be compared. In this manner, it filters out the high frequency noise and thus neglects the deformations of a measurement signal, relative to other signal's, whose spectrum is very close to that of the reference signal. Hence, this algorithm may be applied, in some cases, as an alternative to Fourier transformation or matched filtering.

Moreover this algorithm does not require any modelling of the measurement signals or of the system from which they come. Hence, two major sources of errors are avoided, which

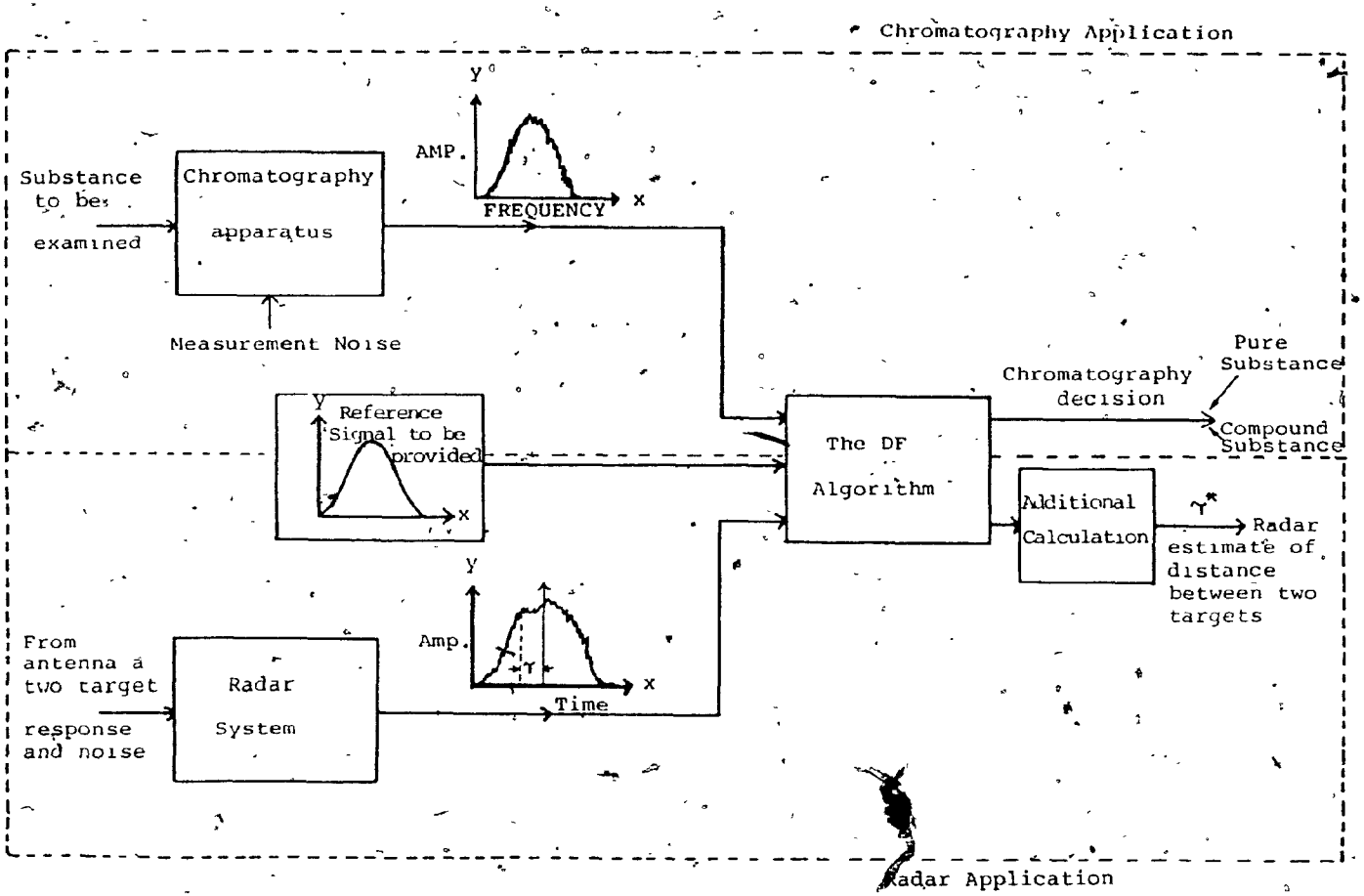

FIGURE 1.1: APPLICATIONS OF THE DF ALGORITHM

are usually encountered in the parameter fitting of the model on the basis of observations. These two sources of error are:

(i) the problem of difference between the fitted model and reality,

(ii) the measurement noise which causes the error in parameter estimation.

The first source of error is absent from the DF algorithm, as it does not require any model. The second type of error is minimized, because normalized integrals are employed.

The other major feature of the DF algorithm is that, it is sensitive only to shape variations. In other words, it is insensitive to many parameter variations which do not change shape. In the case of visual similarity of two shapes, these parameters are the ordinate scale, the zero point of the abscissa, and the abscissa scale. This implies that expansion or contraction of the shape by changing the scale on the X or Y axes, does not change the shape of the signal. This insensitivity to scale change on the abscissa permits this algorithm to be used, whereas a deconvolution algorithm, sensitive to the width of the apparatus function, would not be applicable, due to the uncertainty of this width [2].

1.3 Comparison with the Other Existing Methods

There are predominantly two types of existing methods to detect the difference between two signal shapes. The first type of method works on the principle that the shapes are

different if the difference between their models can be proved. To do that, both single peak and double peak models are prepared, and then the one which seems more appropriate according to some criterion, is selected. This method has an advantage over our method as it can give estimates of the parameters which cause deformation in the shape. For example, in the case of double peaks, estimates of separation between the component peaks and their area ratio can be obtained. But if the shape difference is very small, problems arise using this type of method. As said earlier, the problem of difference between the fitted model and the reality can arise and detection results become doubtful because of the uncertainty of parameter estimates. The main reason for the uncertainty of parameter estimates can be explained by the fact that moment estimates of order one and two do not play any part in characterizing the shape. While higher order moments are very sensitive to the shape variation but their calculation is so sensitive to the noise, that they are of doubtful use in detecting small differences in the shapes.

Another type of method uses the notion of shape and calculates invariants. An invariant is a number which is determined from a particular profile, and depends in reality on the shape of this profile. The above property is applied in the "slope analysis method", in which the ratios between the extreme values taken from the second derivative of the front and the back side of a peak are calculated (exponentially

modified Gaussian [3]). Another example is that of the "method of moments", which uses the relationship between the central moments of order 2, 3 and 4 of a peak [4].

The following criticism may be made regarding these methods. First, they are very sensitive to noise. Second, as invariants are calculated from signal models, they may be inadequate, due to model inaccuracy. Finally, invariants do not characterize the shape, while the DF algorithm uses an invariance property which characterizes the shape.

1.4 The Criterion for Choice of Method

The criterion for choice of a suitable method must be based on following three factors:

(i) The complexity of the method and the resources available. The DF algorithm is quite complex in itself and requires a computer system of modest resources to simulate the algorithm. The other methods appear to be less complex.

(ii) The degree of deformation (shape difference) between the signals and whether parameters of deformation are required. As the DF algorithm does not give estimates for parameters, it should not be used in a case where these parameters are required to be known. However, for detecting a very small degree of deformation, the DF algorithm appears to be the best choice.

(iii) The signal-to-noise ratio of the measurement signal. As the DF algorithm uses normalized integrals to filter out the noise, it may work satisfactorily for lower signal-to-noise ratios, compared to the other methods.

As an addition to the above factors, the following statement can be made: If we have to distinguish, in a noisy environment, a pure peak from another one, apparently unique, but in reality contaminated by a secondary peak in a very small proportion, the DF algorithm is the only one to establish the distinction.

1.5 Possible Applications

There are a number of application areas which can take advantage of this algorithm, as mentioned below.

(i) This algorithm can be applied to the case of:

a) emission or absorption of spectra of electromagnetic waves, a single peak representing a pure line,

b) Lorentzian profiles of light scattering in a transparent environment, a single peak representing one kind of scattering particles,

c) chromatographic peaks, a single peak representing a pure substance.

The above mentioned applications, in general have been dealt-with, using the DF algorithm in Chapter 2 of this work. The results obtained by computer simulation are also presented.

(ii) This algorithm can also be applied to a pattern recognition problem, concerned with spatial recognition of similar 3-dimensional objects or multi-dimensional regions in an image or in a scene.

(iii) To measure the distance between two closely spaced point targets in a radar system. This specific application is implemented and described in Chapter 3.

CHAPTER 2

PRESENTATION OF THE DISTRIBUTION FUNCTION (DF) ALGORITHM

2.1 Introduction

The DF algorithm assists us in making a distinction between two signals which look alike to the naked eye, i.e., those for which there is a very small difference in shape [4]. Using this algorithm we can also decide whether the signal which is measured, the measurement signal, is a pure signal (single peak) or a mixed signal. The latter composite signal may arise when more than one signal are overlapped to the extent that the resultant signal looks like a pure signal having a single peak.

Let the functions describing the signals be real, continuous, positive, and integrable from $-\infty$ to $+\infty$. These properties allow us to compare two signals in the form of functions which are proportional to their probability density functions (p.d.f.).

2.2 Construction of a "Mixed" Measurement Signal

Let the signals which satisfy the above required properties be assumed to be of Gaussian shape. Assume two Gaussian signals, $v_1(t)$ and $v_2(t)$, are the component signals of a mixed or composite signal $v_c(t)$ [2], shown in Figure 2.1 and expressed as,

$$v_c(t) = \alpha\, v_1(t) + (1-\alpha)\, v_2(t) \qquad (2.1)$$

where α is the factor depending upon the ratio of peak amplitudes of both signals, and is called the "proportionality factor". For example, $\alpha = 0.5$ implies that the amplitude of both component signals are the same, or in other words, their distribution has the same standard deviation.

Here $v_1(t)$ and $v_2(t)$ can be represented by the functional form of the Gaussian probability density function [5], as shown in Figure 2.2 and given by,

$$v_1(t) = \frac{1}{\sqrt{2\pi\sigma_1}} e^{-\frac{(t-\theta_1)^2}{2\sigma_1^2}} \tag{2.2}$$

$$v_2(t) = \frac{1}{\sqrt{2\pi\sigma_2}} e^{-\frac{(t-\theta_2)^2}{2\sigma_2^2}} \tag{2.3}$$

where θ_i, σ_i are the mean value and standard deviation, respectively, of $v_i(t)$ $\quad i = 1,2$.

The first non-central moment or mean, μ_{vc}, of the combined signal may be computed as [5],

$$\mu_{vc} = \alpha\,\theta_1 + (1-\alpha)\,\theta_2 \tag{2.4}$$

If we let
$$\begin{aligned} m_1 &= \theta_1 - \mu_{vc} \\ m_2 &= \theta_2 - \mu_{vc} \end{aligned} \tag{2.5}$$

The standard deviation of the combined signal may be calculated as

$$\sigma_{vc} = [\alpha(\sigma_1^2 + m_1^2) + (1-\alpha)(\sigma_2^2 + m_2^2)]^{1/2} \tag{2.6}$$

2.3 Construction of the Reference Signal

To implement the Distribution Function Algorithm, we must construct a "Reference Signal" which is also real, continuous, positive, and integrable from $-\infty$ to $+\infty$. The reference signal is required because in the method we need to compare the "distribution function" of the measurement signal to that of the reference signal.

With the help of the parameters obtained in Section 2.2, i.e., μ_{vc} and σ_{vc}, we will make a pure (single peak) reference signal, which looks like the mixed signal in shape and has the same mean value as the combined signal, but with a standard deviation slightly different than that of the combined signal. A reference signal for certain parameter values of interest is shown in Figure 2.3. We set the mean of the reference signal to be,

$$\mu_r = \mu_{vc}$$

and the standard deviation of the Reference Signal to be,

$$\sigma_r = \sigma_{vc} - \delta$$

where δ is very small in comparison to σ_{vc}. It may be assigned 2 to 3 percent of the value of σ_{vc}.

Then the Reference Signal $s_r(t)$ can be represented by,

$$s_r(t) = \frac{1}{\sqrt{2\pi}\sigma_r} e^{\frac{-(t-\mu_r)^2}{2\sigma_r^2}} \qquad (2.7)$$

2.4 Construction of a Pure (Single Peak) Measurement Signal

Now we will construct another measurement signal which is pure, i.e. represents only one signal, but has the same mean and variance as that of the combined signal. We set the mean of the pure measurement signal as

$$\mu_{vp} = \mu_{vc}$$

and the standard deviation as $\sigma_{vp} = \sigma_{vc}$. So, this signal can be represented in the following way,

$$v_p(t) = \frac{1}{\sqrt{2\pi}\,\sigma_{vp}} e^{-\frac{(t-\mu_{vp})^2}{2\sigma_{vp}^2}} \qquad (2.8)$$

and is shown in Figure 2.4.

2.5 Adding Noise to the Measurement Signals

Signals constructed in the above fashion are the ideal measurement signals, i.e., without any noise. But in communication or pattern recognition systems, signals are contaminated because of the presence of noise added to the incoming signals. So to construct the actual signals, we add white noise with mean zero and a standard deviation depending upon the signal-to-noise ratio. A derivation for the computation of the standard deviation of the noise as a function of desired signal-to-noise (S/N) ratio is shown in Appendix 1.

Let σ_n be the standard deviation of the white noise, for a particular S/N ratio. To construct the noise, we use a Uniform Random Number Generator. These noise samples have

values lying between 0 and 1 and have distribution with a mean value of 0.5 and standard deviation of $\sqrt{1/12}$. Then uniform random noise samples with mean zero and a prescribed standard deviation σ_n can be represented as,

$$n(t) = (\text{RANF}\ (1) - 0.5) \times \sqrt{12} \times \sigma_n \qquad (2.9)$$

where RANF (1) is the 'Computer Library Function', which gives the uniformly distributed numbers between 0 and 1.

Adding these noise samples to our measurement signals, we obtain the desired noisy signals:

$$\text{Combined Noisy Signal: } nv_c(t) = v_c(t) + n(t)$$
$$\text{and pure Noisy Signal: } nv_p(t) = v_p(t) + n(t) \qquad (2.10)$$

Typical curves for these signals are shown in Figures 2.5 and 2.6, respectively.

2.6 Applying the Method

Now that we have constructed all the signals required, we are ready to apply the Distribution Function method for detection of the shape difference between two potentially different signals.

The first step is to compute the distribution function of all the three signals previously constructed.

The Distribution Function of the reference signal is given by,

$$S_r(x) = \frac{\int_{-\infty}^{x} s_r(t)\, dt}{\int_{-\infty}^{\infty} s_r(t)\, dt} \qquad (2.11)$$

As a function, $s_r(t)$ is a positive p.d.f., (because of its properties), $S_r(x)$ has the properties of a continuous and increasing distribution function (df). Thus, the function $S_r(x)$ also has an inverse function, $S_r^{-1}(x)$.

Similarly, the distribution functions of the noisy combined signal and the noisy pure signal can be represented, respectively, as,

$$V_c(x) = \frac{\int_{-\infty}^{x} n\, v_c(t)\, dt}{\int_{-\infty}^{\infty} n\, v_c(t)\, dt} \qquad (2.12)$$

and

$$V_p(x) = \frac{\int_{-\infty}^{x} n\, v_p(t)\, dt}{\int_{-\infty}^{\infty} n\, v_p(t)\, dt} \qquad (2.13)$$

The definition of <u>shape constancy</u> of the signal $s_r(t)$ depends upon the following property of $S_r(x)$.

The function $S_r(x)$ is invariant for any transformation of $s_r(t)$ of the type,

$$s_r(x) \rightarrow v(x) = K\, s_r[\phi^{-1}(x)]\, \frac{d}{dx}\, [\phi^{-1}(x)] \qquad (2.14)$$

where K is a positive constant, $\phi(\cdot)$ is an increasing continuous function, and $v(x)$ can be either $v_c(x)$ or $v_p(x)$. The last factor in Equation (2.14) is the Jacobian of the transformation. It can be proved that the distribution function $S_r(x)$ and $V(x)$ are equal at points x and y related by

$$y = \phi(x) \text{ or,}$$

$$S_r(x) = V(y) = V[\phi(x)]$$

The relation between $S_r(x)$ and $V(x)$ can be rewritten from the above as,

$$V^{-1}[S_r(x)] = \phi(x) \qquad (2.15)$$

This is the invariance property of the distribution function and can be used to define the invariance in shape of the signals.

2.6.1 Construction of the Function ϕ

When comparing the distribution function of the reference signal $s_r(t)$ to the distribution function of the measurement signal, the comparison leads to a point-by-point construction of the function $\phi(x)$ defined in the following manner. For a combined (measurement) signal,

$$\phi_c(x) = V_c^{-1}[S_r(x)]$$

and for a pure (measurement) signal,

$$\phi_p(x) = V_p^{-1}[S_r(x)]$$

The above relationship is equivalent to,

$$V[\phi(x)] = S_r(x).$$

Computing the equation,

$$V(y) = S_r(x)$$

where $V(y)$ may be either $V_c(y)$ or $V_p(y)$, allows the function $y = \phi(x)$ to be determined.

We use a constant increment on the ordinate for the distribution function $S_r(x)$ and $V(y)$. Thus, in reality two equations are solved,

$$S_r(x) = i/n$$
$$\text{and} \qquad V(y) = i/n \tag{2.16}$$

where n is the number of sample points of the ordinate, i is an integer ranging from 1 to n. Two typical curves for the function $\phi(\cdot)$ are shown in Figures 2.7 and 2.8. Figure 2.7 is obtained by comparing the reference signal to the combined measurement signal; whereas, Figure 2.8 is obtained by comparing the reference signal to the pure measurement signal, for a fixed signal-to-noise ratio.

2.6.2 The Detection Criterion

While constructing the function $\phi(x)$, we obtain the points x_i and y_i, $i = 1,2,\ldots,n$, on the x and y axes respectively. In our case of visual similarity between two signals, the deviation of $\phi(x)$ from linearity will be measured.

We fit a curve to the above data for $\phi(x)$ by using the method of least squares [6] with the parabolic regression equation,

$$y = \beta_o + \beta_1 x + \beta_2 x^2$$

where β_2 is a measure of deviation of the curve $\phi(x)$ from linearity, i.e. $\beta_2 = \frac{d^2y}{dx^2}$, the curvature. As derived in Appendix 2, β_2 can be easily calculated from the points (x_i, y_i) $i = 1,2,\ldots,n$.

We calculate β_2 separately, first comparing the reference signal to the pure measurement signal, and then comparing the reference signal to the combined measurement signal.

With a number of pure measurement signals compared with reference signals, we obtain different values of β_2, e.g., $(\beta_2)_1$, $(\beta_2)_2$, $(\beta_2)_3$..... Let the maximum difference between two extreme values of β_2 so obtained be,

$|(\beta_2)_{max}| - |(\beta_2)_{min}| = d_o$, if both β_2 are of same sign.

or

$|(\beta_2)_{max}| + |(\beta_2)_{min}| = d_o$, if both β_2 are of opposite sign

Now, in actual application, we have,

$|(\beta_2)_{measurement}| - |(\beta_2)_{min}| = d$, if both β_2 are of same sign

$|(\beta_2)_{measurement}| + |(\beta_2)_{min}| = d$, if both β_2 are of opposite sign.

and if $d > k\, d_o$, where $k = 2$ for example, then we can say, the measured signal is a combined signal; otherwise, we say it is a pure (single peak) signal. Here $k\, d_o$ is the threshold value which depends on the desired probability of classification error and upon the signal-to-noise ratio existing on the signal recordings to be compared. So in a specific case this value can be fixed by the S/N ratio and the possible deformation expected.

2.7 Simulation of Algorithm

In this section the DF algorithm is computer simulated. Data required to construct the reference and the measurement signals are chosen to provide meaningful comparisons.

Let,

- the mean value of the component 1 of the combined measurement signal, $\theta_1 = 2.27$;
- the mean value of the component 2 of the combined measurement signal, $\theta_2 = 1.82$;
- the standard deviation of the reference signal, $\sigma_r = 0.39$; and
- the proportionality factor $\alpha = 0.5$.

The following tables were made, running the computer program each time to determine the value of β_2.

Table 2.1: Values of β_2, obtained when the measurement signal is pure (single peak).

Standard deviation of measurement signal	Measurement signal with no noise	Measurement signal with noise	
		S/N = 20dB	S/N = 25dB
0.40	$-.343 \times 10^{-3}$	$-.972 \times 10^{-3}$	$-.719 \times 10^{-4}$
0.41	$-.395 \times 10^{-3}$	$-.474 \times 10^{-4}$	$-.483 \times 10^{-3}$
0.42	$-.359 \times 10^{-2}$	$-.186 \times 10^{-2}$	$-.235 \times 10^{-2}$

Table 2.2: Values of β_2, obtained when the measurement signal is combined (composite peak).

Standard deviation of measurement signal	Measurement signal with no noise	Measurement signal with noise	
		S/N = 20dB	S/N = 25dB
0.40	$-.1373 \times 10^{-1}$	$-.217 \times 10^{-2}$	$-.4515 \times 10^{-2}$
0.41	$-.1302 \times 10^{-1}$	$-.373 \times 10^{-2}$	$-.6201 \times 10^{-2}$
0.42	$-.1392 \times 10^{-1}$	$-.414 \times 10^{-2}$	$-.7742 \times 10^{-2}$

Choosing the case only for signal-to-noise ratio equal to 25 dB, from Table 2.1, we have

$$d_o = .235 \times 10^{-2} \sim .719 \times 10^{-4} = .2278 \times 10^{-2}$$

From table 2.2 we have,

$$d = .4515 \times 10^{-2} - .719 \times 10^{-4} = .4443 \times 10^{-2}$$

Here we see that $d \neq 2d_o$, and we can decide that the measurement signal is a combined signal.

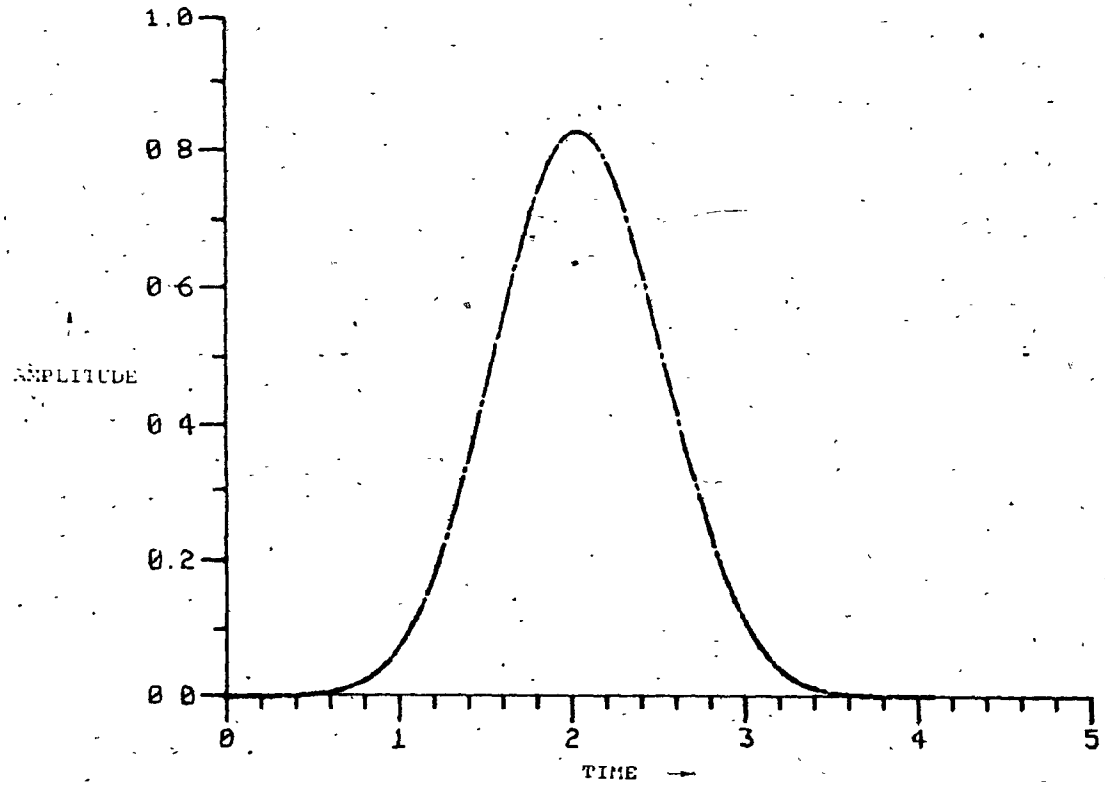

FIGURE 2.1: MIXED MEASUREMENT SIGNAL

$\mu_1 = 2.27$ $\mu_2 = 1.83$
$\sigma_1 = 0.42$ $\sigma_2 = 0.42$

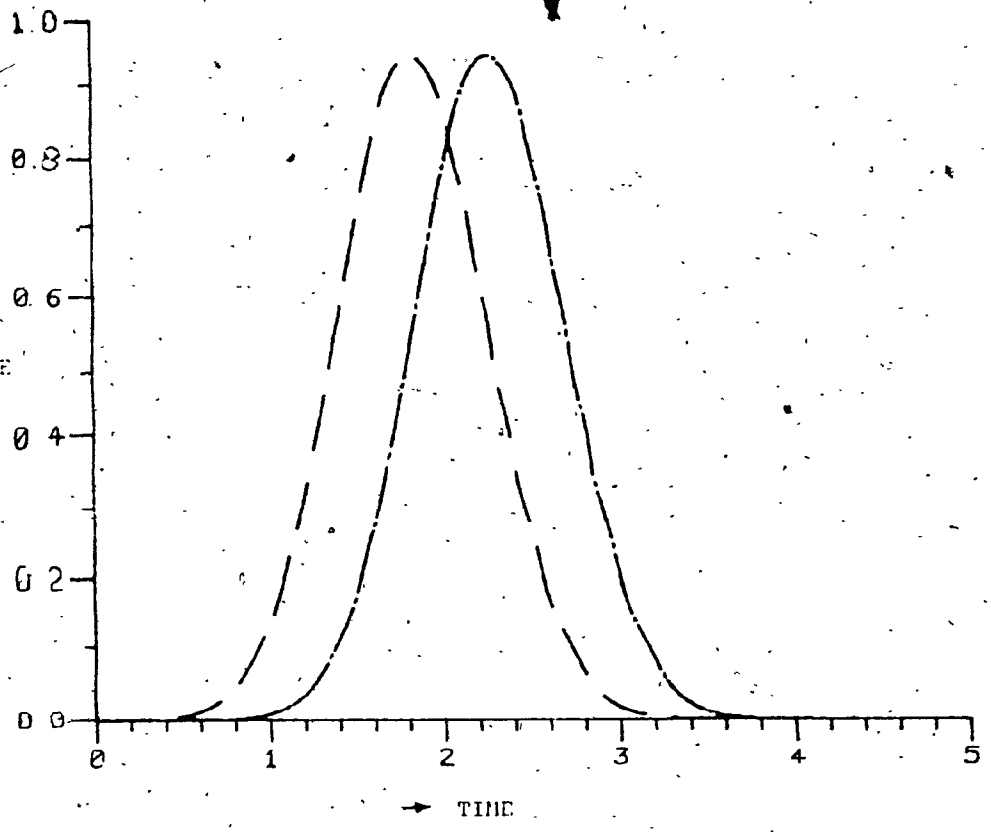

FIGURE 2.2: COMPONENTS OF THE MIXED SIGNAL

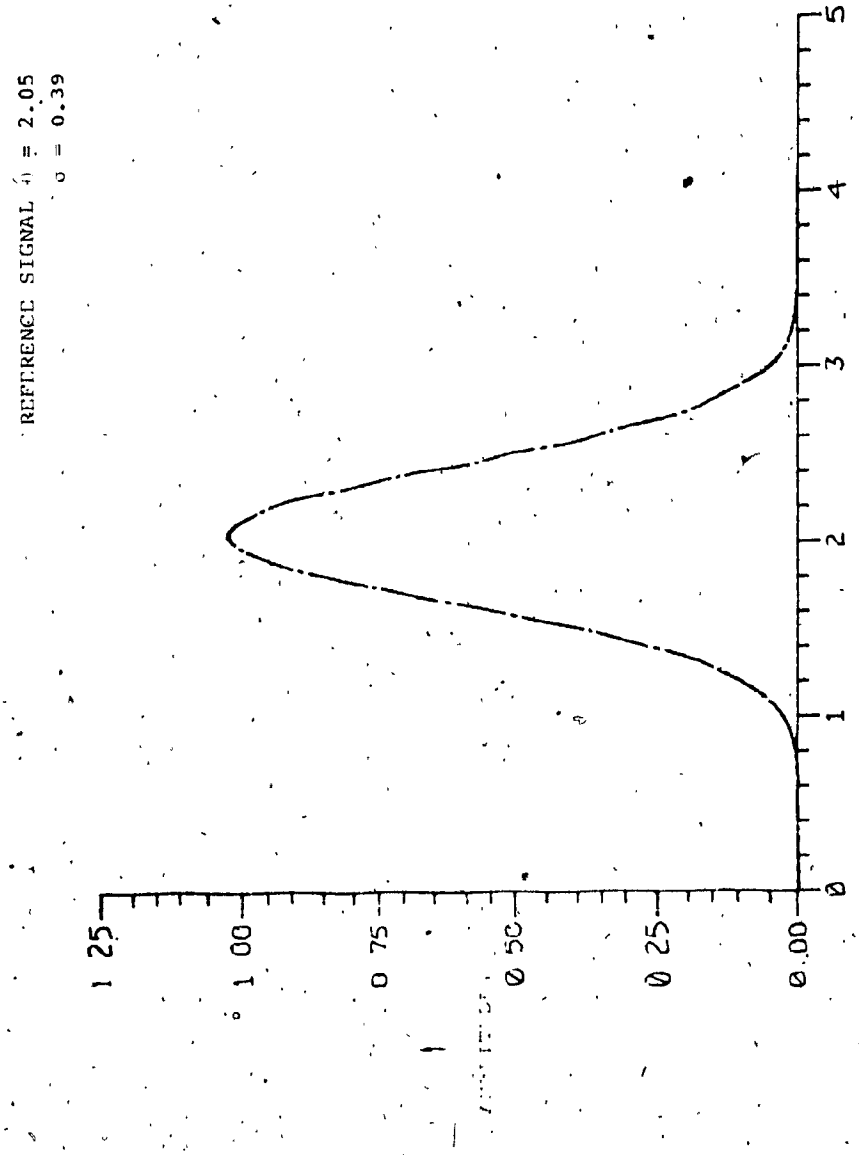

FIGURE 2.3: THE REFERENCE SIGNAL

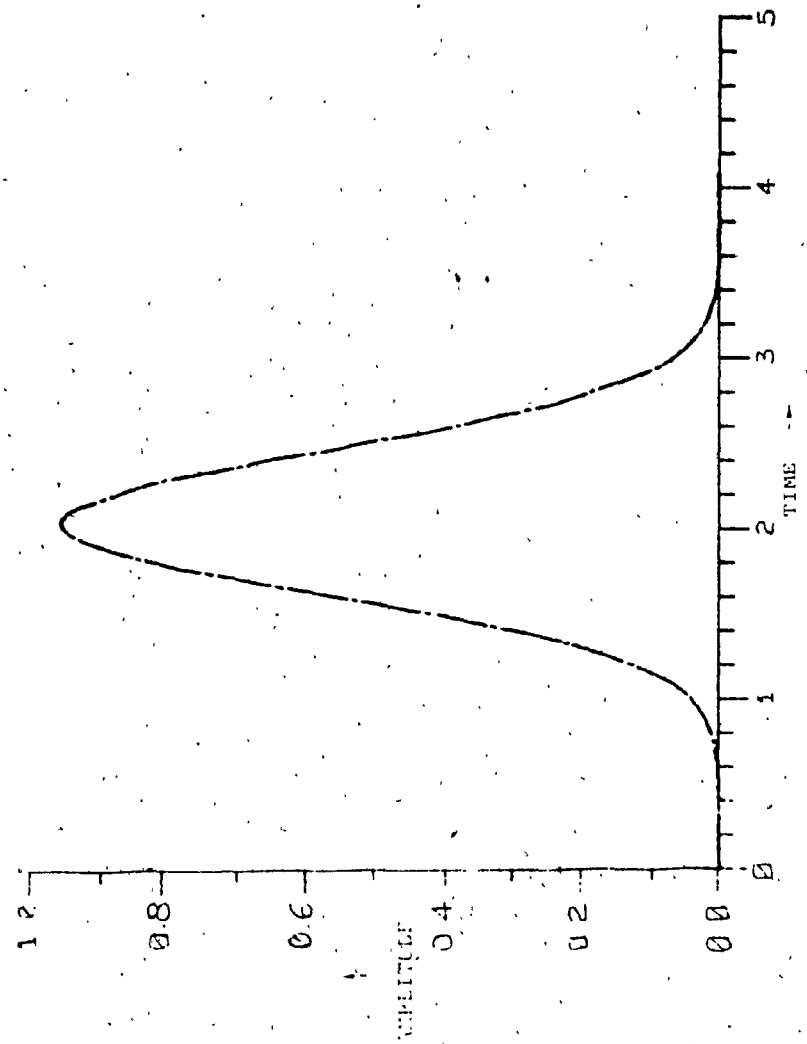

FIGURE 2.4: PURE MEASUREMENT SIGNAL (SINGLE PEAK)

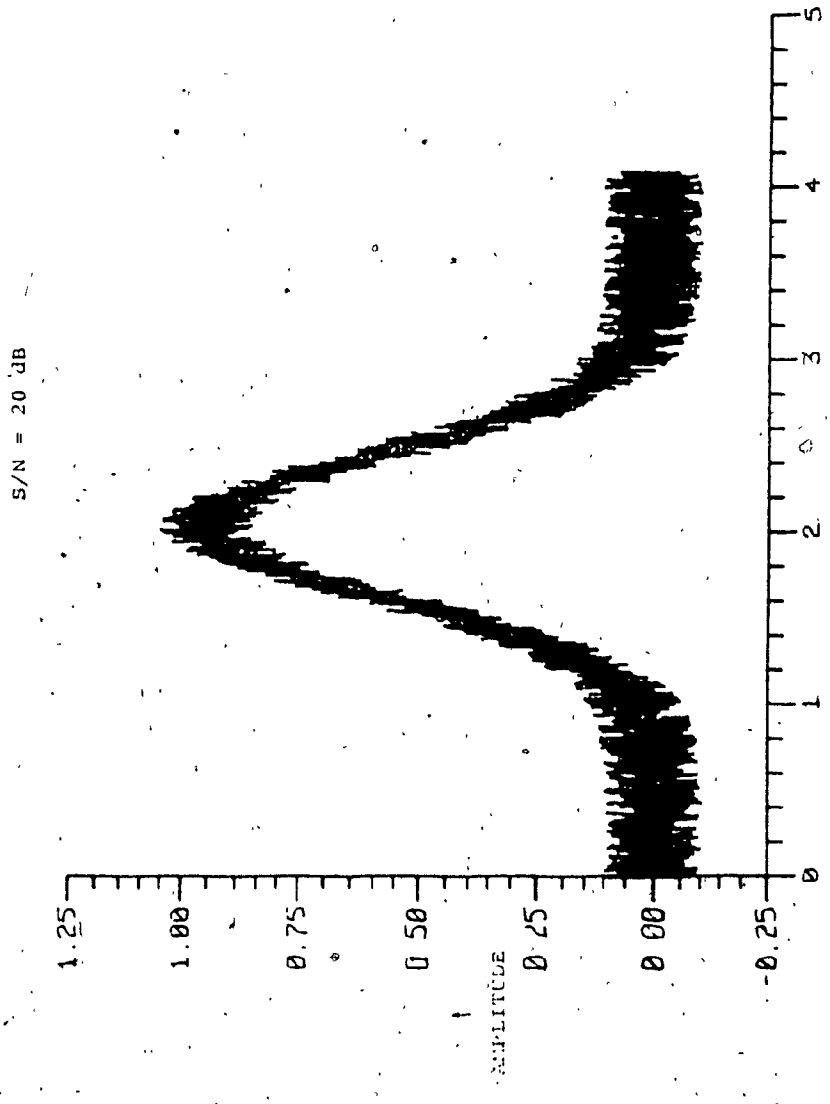

FIGURE 2.5: MIXED MEASUREMENT SIGNAL WITH NOISE

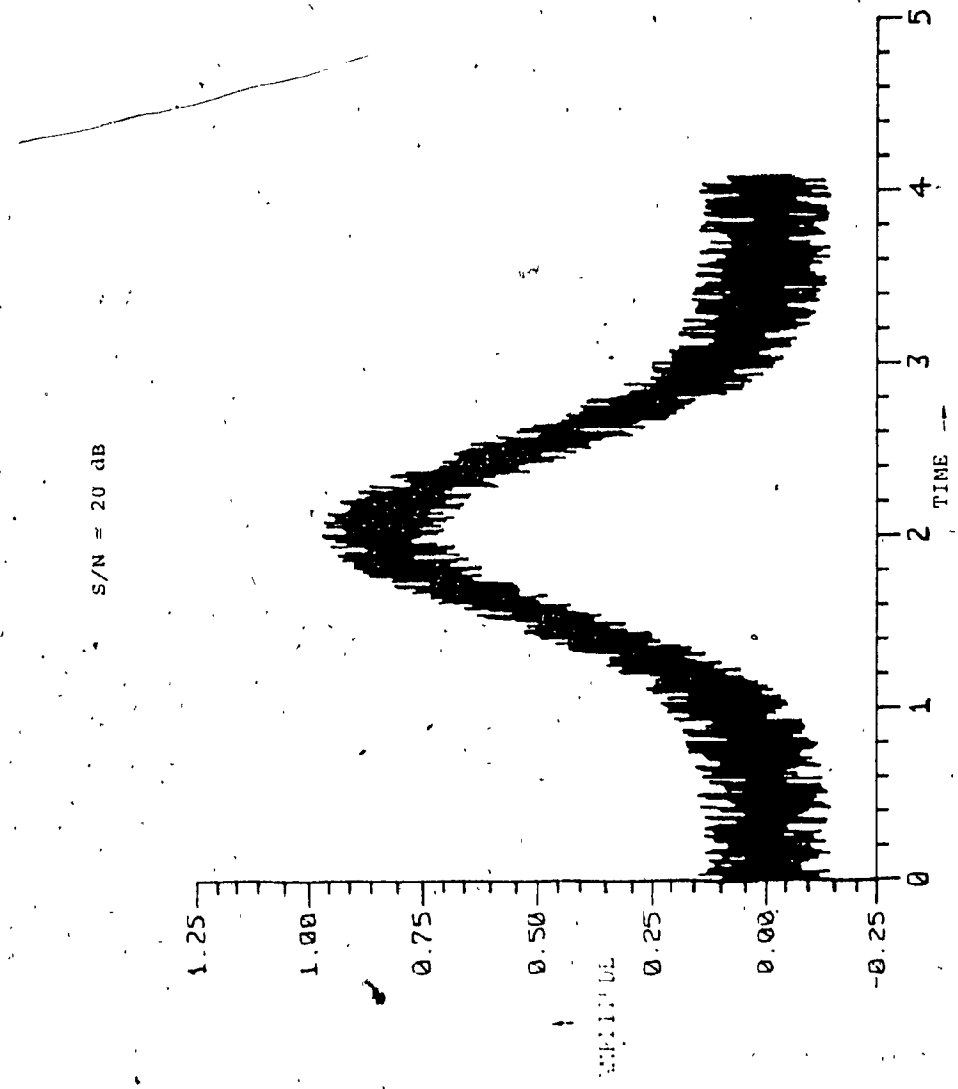

FIGURE 2.6: PURE MEASUREMENT SIGNAL WITH NOISE

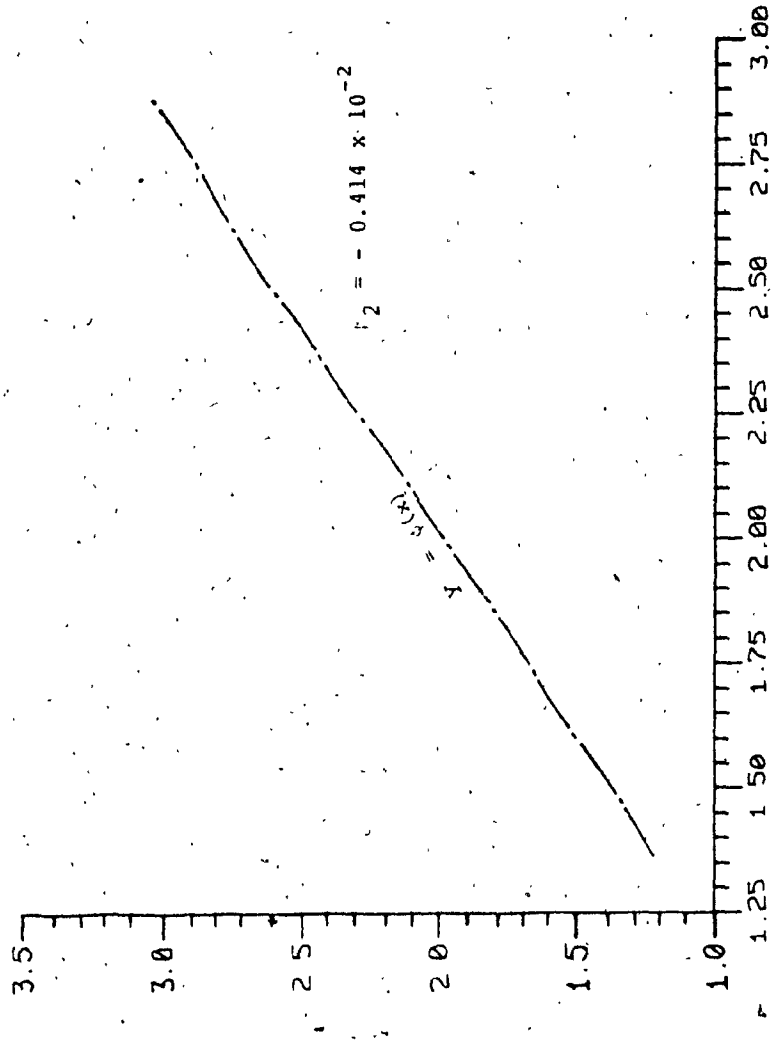

FIGURE 2.7: FUNCTION ψ FOR NOISY MIXED MEASUREMENT SIGNAL

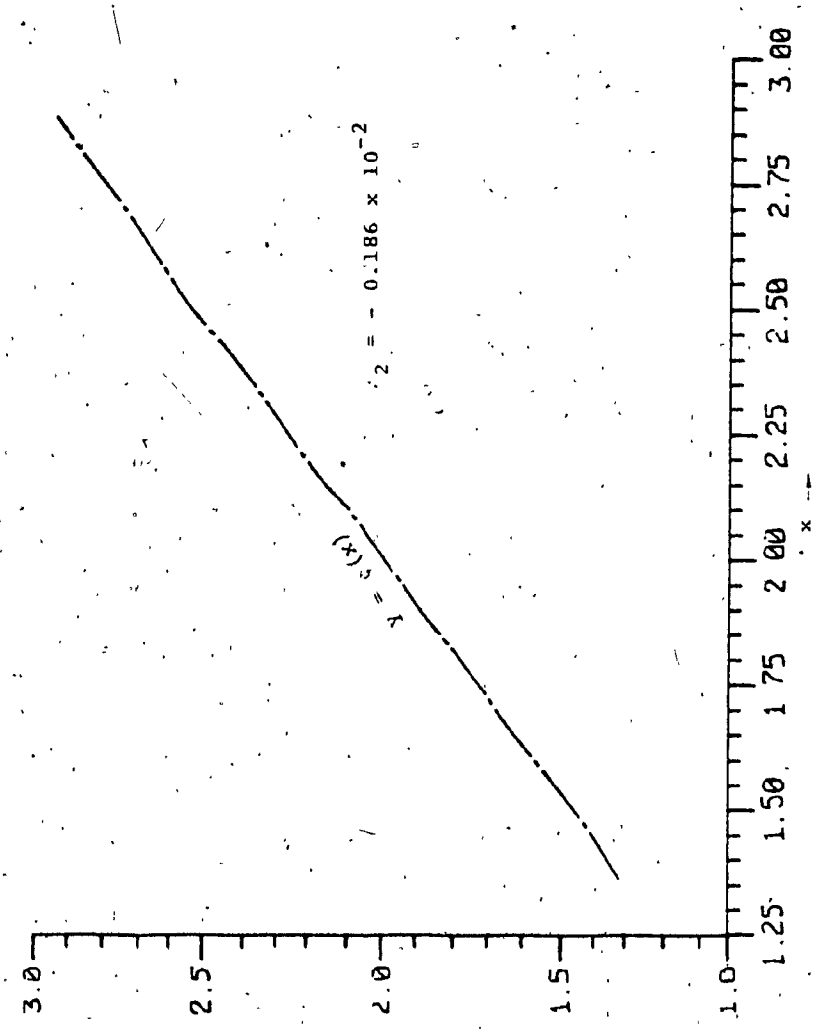

FIGURE 2.8: FUNCTION ζ FOR NOISY FURE MEASUREMENT SIGNAL

If the difference between θ_1 and θ_2 is increased, we can get equally good results at lower signal-to-noise ratios.

Figures 2.1 to 2.8 are plotted on the computer graphics machine for a particular case from the above table. Figure 2.1 represents the combined measurement signal. In Figure 2.2 the components of the combined measurement signal are shown. Figure 2.3 is obtained for the pure reference signal. Figure 2.4 shows the pure measurement signal. Figures 2.5 and 2.6 are obtained on adding the measurement noise to the signals of Figure 2.1 and 2.4 respectively. Lastly, the function ϕ for the noisy combined signal and the noisy pure signal is shown in Figures 2.7 and 2.8 respectively.

2.8 SOME GENERAL RESULTS

Some general and intersting results of the algorithm in the form of certain curves have been obtained. Basically, the variation of the value β_2 for different values of the ratios θ_2/θ_1, and σ_2/σ_1, is computed and plotted as shown in the Figures 2.9 to 2.12, where θ_1 and θ_2 are the mean values, respectively, of component 1 and component 2 of a combined measurement signal and σ_1 and σ_2 are the standard deviations of the two components. Again, these component signals are assumed to be of Gaussian shape. On the x-axis, we plot the ratio θ_2/θ_1, and on the y-axis, the values of β_2 are plotted. Each figure shows five different curves for different values of the ratio σ_2/σ_1.

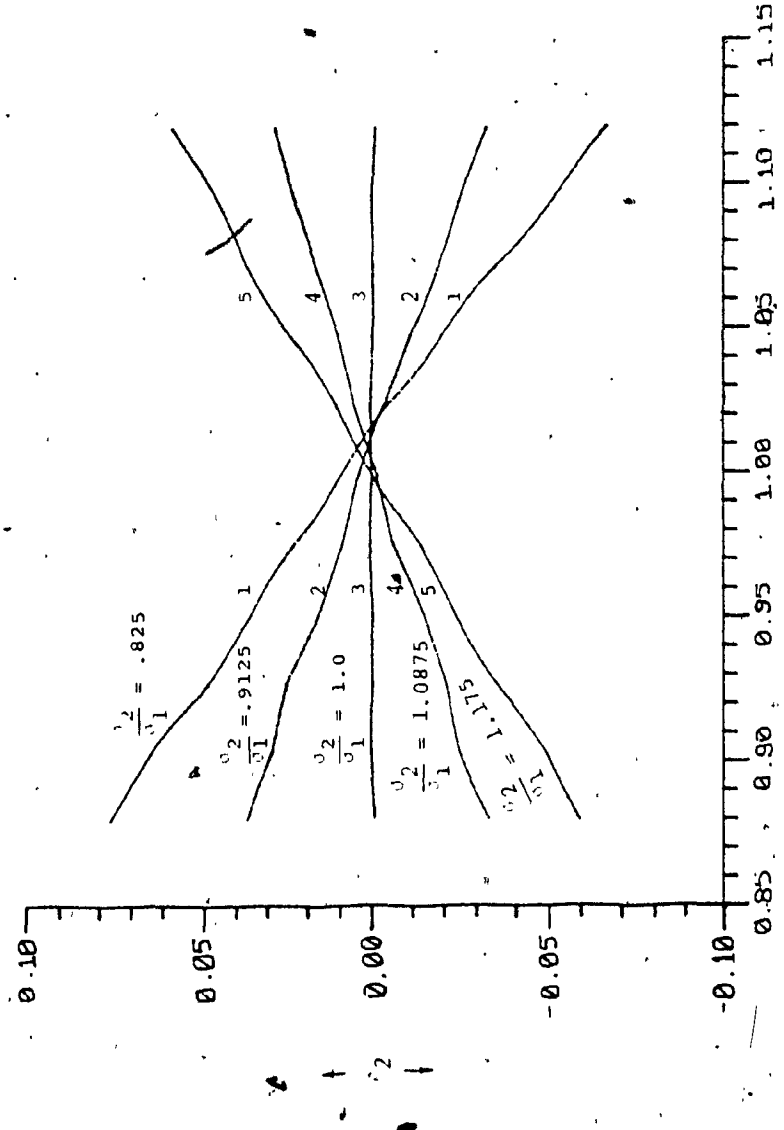

FIGURE 2.9: VARIATION OF ρ_2 FOR MIXED SIGNAL WITHOUT NOISE

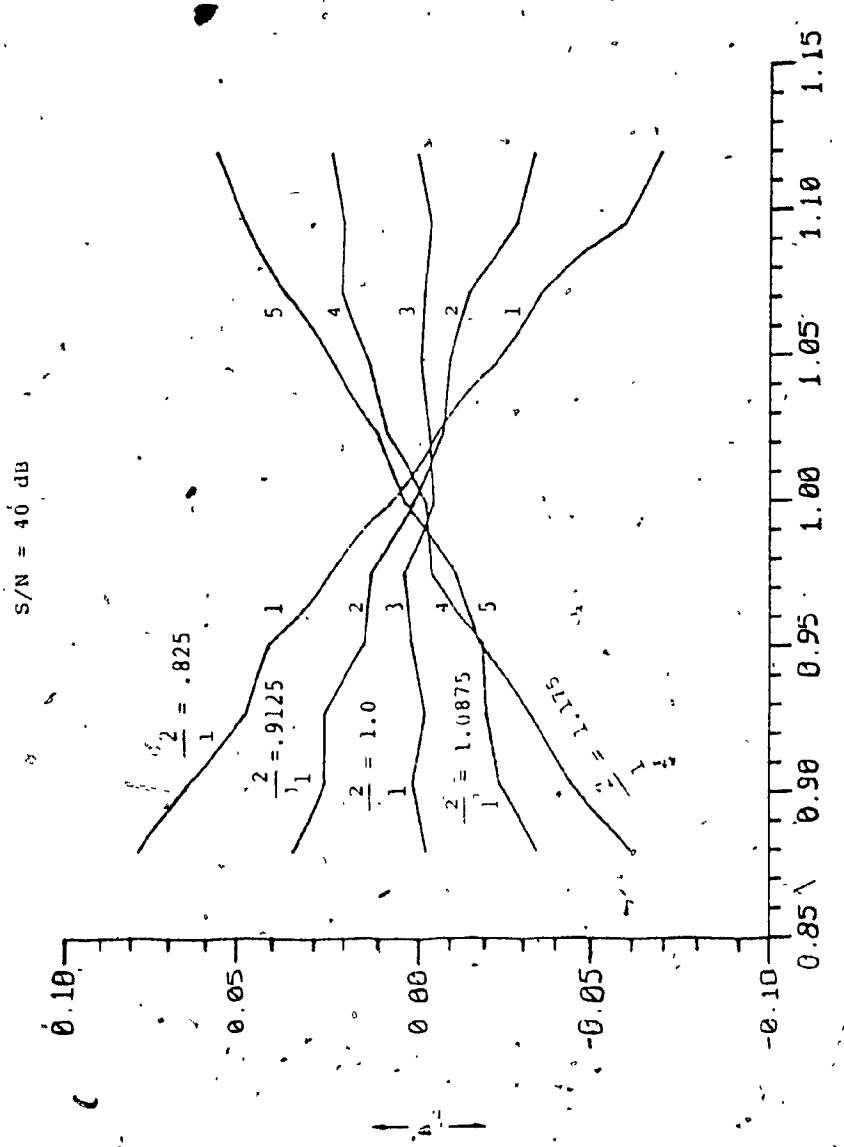

FIGURE 2.10: VARIATION OF ℓ_2 FOR MIXED SIGNAL WITH NOISE

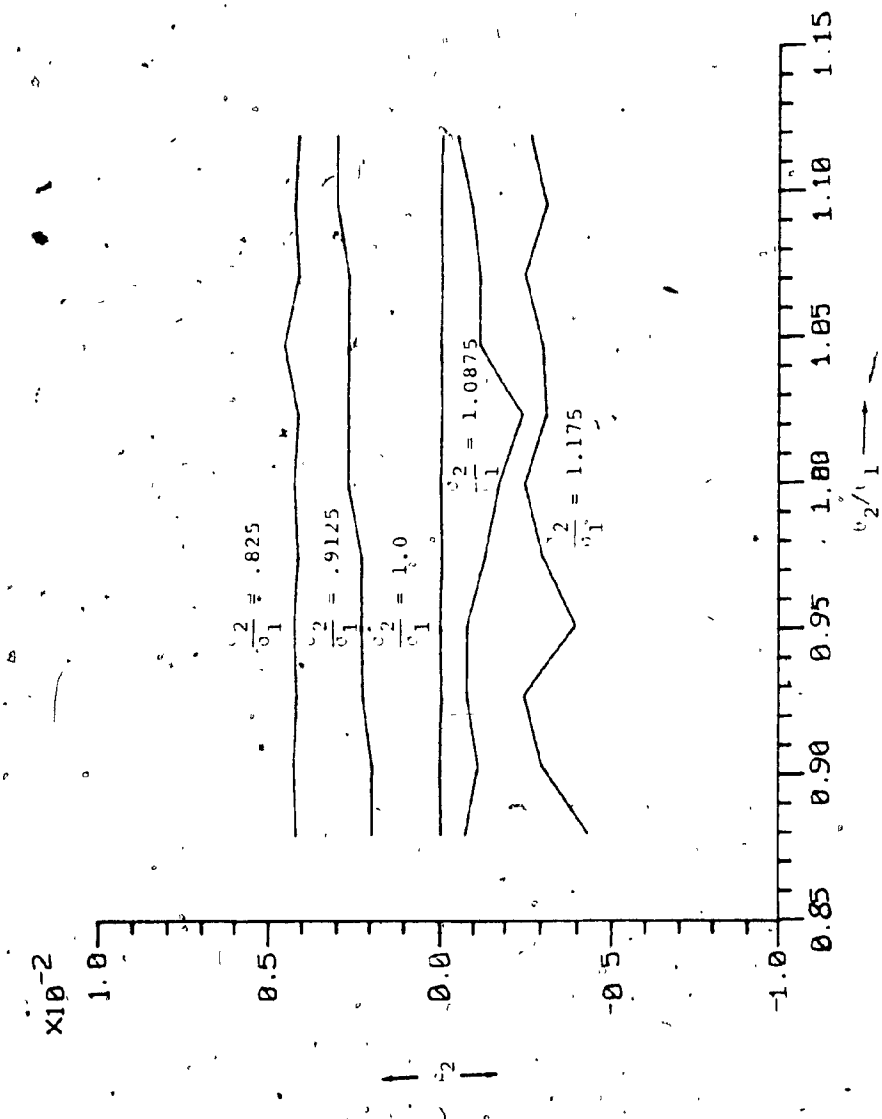

FIGURE 2.11: VARIATION OF β_2 FOR PURE SIGNAL WITHOUT NOISE

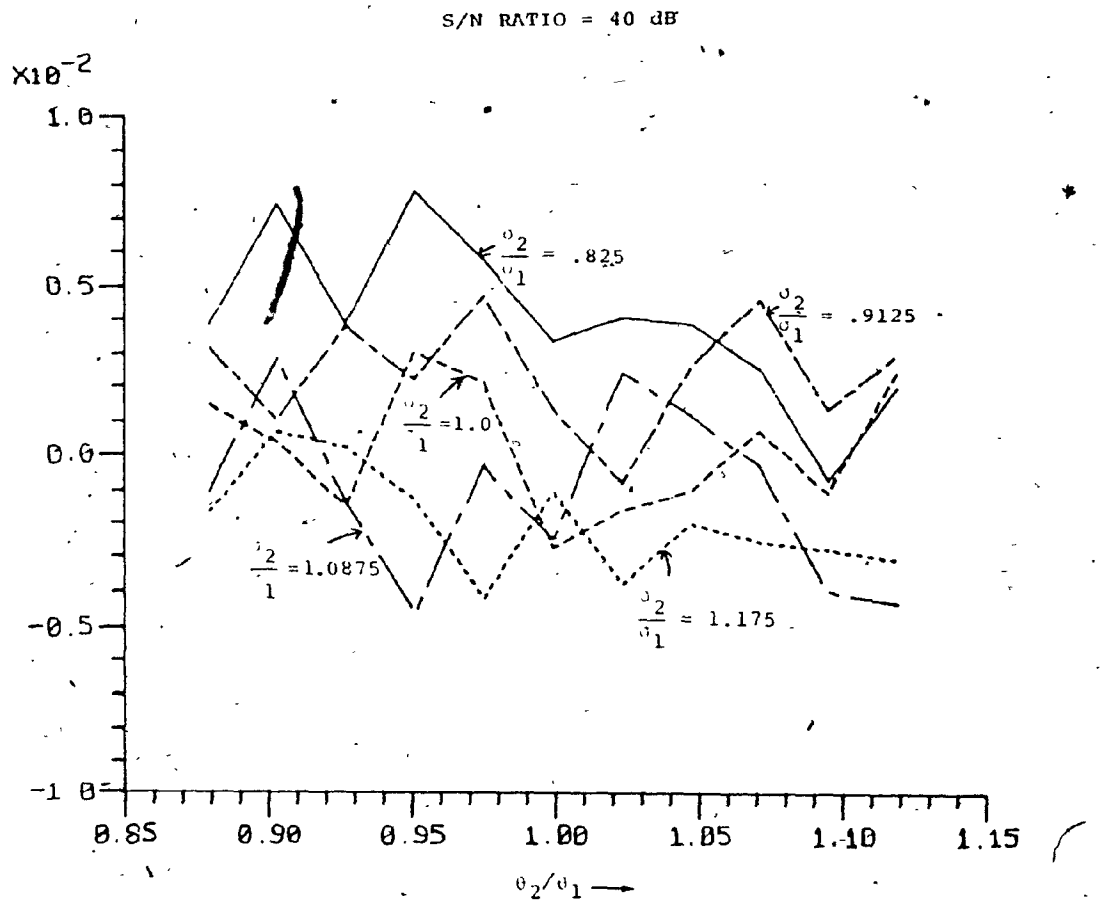

FIGURE 2.12: VARIATION OF β_2 FOR PURE SIGNAL WITH NOISE

While applying the DF algorithm, component 1 of the combined signal is kept constant with the mean value 2.08 and the standard deviation equal to 0.4. These values have been selected arbitrarily. To obtain the different curves, the mean value and the standard deviation of component 2 are changed, and the value of β_2 computed each time. Here component 1 is used as the reference signal. Two sets of the results are prepared. One, considering the measurement signal as a combined signal and the other, when the measurement signal is a pure signal (with equivalent values of the mean and the standard deviation). Figures 2.9 and 2.11 are prepared for a measurement signal without any measurement noise. Figures 2.10 and 2.12 represent the case when the measurement signal is noisy, the signal-to-noise ratio being equal to 40 dB.

On observing these curves, the following conclusions about the results can be made:

(1) The values of $|\beta_2|$ are significantly higher for the combined measurement signal than the values obtained for the pure measurement signal.

(2) As the distance between the mean values of the two components increases, the $|\beta_2|$ value also increases while measuring the combined signal. But in the case of the pure measurement signal, theoretically the $|\beta_2|$ value does not change as the mean value of the signal changes. Actually in Figure 2.11, the curves should

be horizontal straight lines, but are difficult to obtain, because of the fineness of quantization along the Y-axis.

(3) The value of $|\beta_2|$ increases, as the ratio σ_2/σ_1 deviates from unity, indicating more deformation in the shape of the measurement signal.

CHAPTER 3

APPLYING THE DF ALGORITHM TO A MULTI-TARGET RADAR PROBLEM

3.1 Introduction

In this chapter we apply the DF algorithm to measuring the distance between two closely spaced point targets in a radar system. We calculate the root-mean-square (r.m.s.) error in measurement of distance using this algorithm and compare it to the conventional threshold and moment algorithms [7], which are presently employed for this purpose.

In radar systems a pulse of known shape with a peak amplitude depending upon the radar cross section (RCS) of the target is received from each point target. Because of the distance between the two point targets, the pulse returned from the second target is delayed in time and has a phase difference with respect to the first returned pulse. In the receiver these two returned pulses are added vectorially to form a combined two target response. As this response is a complex function in nature, we will consider its absolute value when applying the method.

3.2 Constructing the Measurement Signal for the Combined Two Point Target Response

We model each point target returned pulse as having a Gaussian pulse shape. For convenience, the notation for a few parameters involved are changed from those used in Chapter 2. Let θ_1 and θ_2 be the mean of the first and second pulses,

respectively, and σ_p be the rms value of the Gaussian pulse shape. To normalize the pulse envelope from the point target, the rms pulse width σ_p is set equal to 1. As shown in Figure 3.1 let t = 0 be the arbitrary defined mid-point. Then the normalized distance (delay) is given by $\tau = \frac{|\theta 1|}{\sigma_p} = \frac{|\theta 2|}{\sigma_p}$. Thus we can define a normalized pulse spacing or pulse width equal to $2\sigma_p$ The return pulse from each target can be represented as,

$$v_1(t) = 1/\sqrt{2\pi\sigma_p}\ e^{\frac{-[t+\tau]^2}{2\sigma_p^2}} \qquad (3.1)$$

and

$$v_2(t) = 1/\sqrt{2\pi\sigma_p}\ e^{\frac{-[t-\tau]^2}{2\sigma_p^2}} \qquad (3.2)$$

The complex signal of these two pulses, v(t) is of the form,

$$v(t) = \alpha\, v_1(t)\, e^{j\gamma/2} + (1-\alpha)\, v_2(t)\, e^{-j\gamma/2} \qquad (3.3)$$

where γ = Radio frequency (RF) phase difference between two component pulses, and

α = Scattering strength of target, depending upon the peak amplitudes of the individual pulses, which again depend upon the RCS of the targets.

For example, equal RCS of the point targets implies α equal to 1/2. Equation (3.3) can be rewritten as,

$$v(t) = \alpha\, v_1(t)\, [\cos \gamma/2 + j \sin \gamma/2] + (1-\alpha)\, v_2(t)\, [\cos \gamma/2 - j \sin \gamma/2]$$

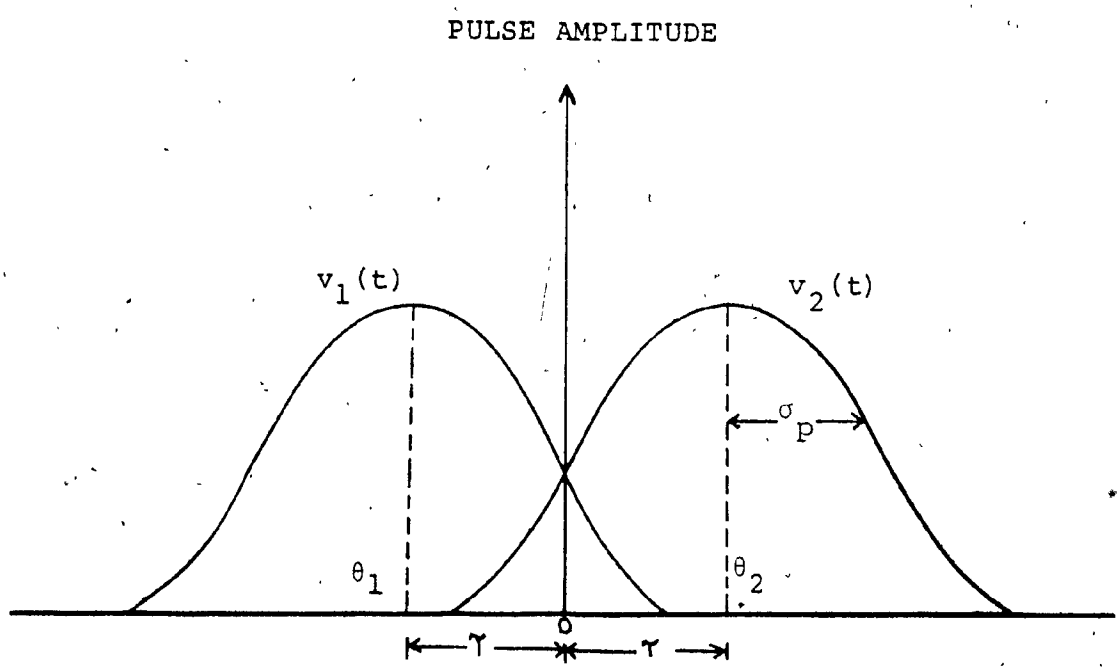

FIGURE 3.1: TWO POINT TARGET RESPONSE

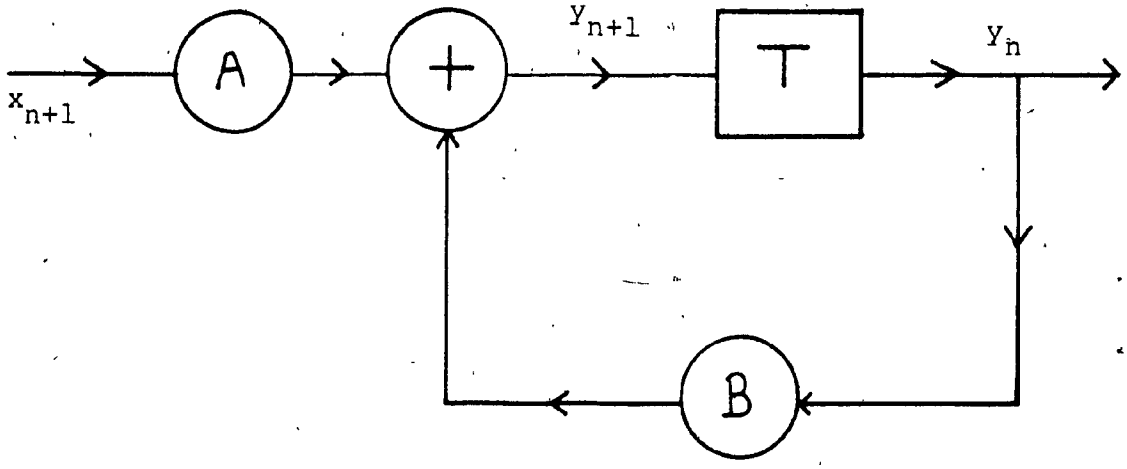

FIGURE 3.2: FIRST ORDER AUTUREGRESSIVE MODEL

or,

$$v(t) = \cos \frac{\gamma}{2} [\alpha v_1(t) + (1-\alpha)\ v_2(t)] + j \sin \frac{\gamma}{2} [\alpha v_1(t) - (1-\alpha)\ v_2(t)] \qquad (3.4)$$

or,

$$v(t) = \mathrm{Re}[v(t)] + j\ \mathrm{Im}[v(t)]$$

The magnitude of $v(t)$ is from (3.4),

$$v(t) = \{(\mathrm{Re}[v(t)])^2 + (\mathrm{Im}[v(t)])^2\}^{1/2} \qquad (3.5)$$

Equation (3.5) describes the combined signal without any noise added to it. To make it a noisy signal, we should prepare two noise records $n_R(t)$ and $n_I(t)$ uncorrelated to each other. These noise samples are produced from random samples with a Gaussian distribution with mean zero and standard deviation fixed for a specified signal-to-noise ratio (Appendix 1). To provide a realistic degree of correlation between noise samples for each noise record, the samples may be passed through a digital filter. As the noisy signal (signal + white noise) is passed through a filter matched to the transmitted signal at the radar station, the signal is passed as such, but the noise is correlated after filtering.

In our computer simulation of the method, we prepare the white noise samples, introduce correlation between them, and add them to the signal. The correlation between the noise samples is dependent upon the cut-off frequency of a digital filter, or in other words, the white noise is band limited, with the band width determined by the cut-off frequency. Noise samples input to the filter are white, in the sense that samples separated in time by at least $1/f_s$ seconds, are statistically independ-

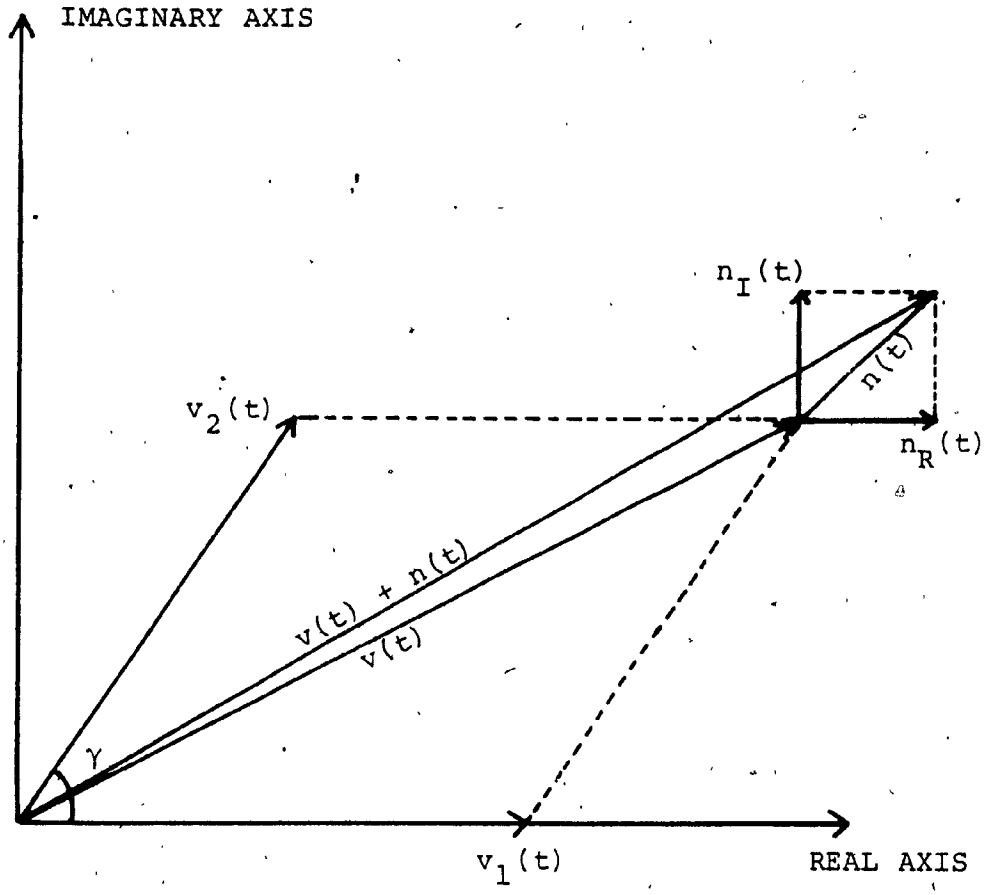

FIGURE 3.3: VECTOR DIAGRAM FOR SIMULATION PROGRAM

ent, where f_s is the sampling rate. After passage through the filter, the time between the statistically independent samples is approximately π/w_c seconds, where w_c is the cutoff frequency of the digital filter. Thus, the number of the output samples which have a significant degree of correlation is approximately $\pi . fs/w_c$.

A first order auto-regressive (AR) scheme is used to introduce the correlation between the white noise samples.

The first order AR equation is,

$$y_{n+1} = B\ y_n + A\ x_{n+1} \qquad (3.6)$$

which can be clearly understood by the block diagram of Fig. 3.2. Here x_n represent white noise samples before filtering and y_n are correlated noise samples after filtering. T is a sample delay which is equal to $1/f_s$. The coefficient B is the multiplying factor which decides the extent of correlation between the noise samples; whereas A, provides a scaling of the input. These factors are the parameters obtained from the transfer function of the equivalent one-pole digital filter, as shown in Appendix 3. These parameters vary as the cut-off frequency of the digital filter is varied.

As shown in Figure 3.3, $n_R(t)$ and $n_I(t)$ are added to the real and imaginary parts of v(t), respectively.

The real part of the noisy measurement signal, $v_N(t)$, is,

$$\text{Re}\ [v_N(t)] = \text{Re}\ [v(t)] + n_R(t) \qquad (3.7)$$

and the imaginary part is,

$$Im[v_N(t)] = Im[v(t)] + n_I(t) \tag{3.8}$$

The magnitude of the noisy measurement signal is given by,

$$|v_N(t)| = \{(Re[v_N(t)])^2 + (Im[v_N(t)])^2\}^{1/2} \tag{3.9}$$

The above expression provides us with the combined noisy measurement signal; noise being added for a certain S/N ratio.

3.3 Constructing the Reference Signal

In this application, the first return pulse from the single point target, is taken as a reference signal. The reference signal is noise-free and given by,

$$s_r(t) = v_1(t) = \frac{1}{\sqrt{2\pi}\sigma_p} e^{\frac{-(t+\tau)^2}{2\sigma_p^2}} \tag{3.10}$$

3.4 Applying the Algorithm

Once measurement and reference signals are obtained, the procedure for determining the deviation of the function Φ from linearity i.e., β_2, is the same as in Chapter 2, which can be summarized in the following steps:

(i) Calculate the distribution function of the measurement signal (both with and without noise), and of the reference signal.

(ii) Construct the function ϕ the first time, comparing the measurement signal (no noise) with the reference signal and, the second time, comparing the noisy measurement signal with the reference signal.

(iii) Calculate β_2(pure) and β_2(noisy) for the no-noise measurement signal, and the noisy measurement signal, respectively.

The absolute value of β_2 is related to the distance between the two point targets. As this distance increases, the absolute value of β_2 increases, and vice-versa, with the relationship between τ (normalized distance) and β_2 being almost linear. In other words, the value of β_2 is a measure of the distance between the two targets. We will take benefit of this fact and determine the distance by calculating the value of β_2.

3.5 Performance of the DF Algorithm

For judging the performance of the DF algorithm, we calculate the normalized r.m.s. error in measuring the normalized distance τ between two point targets. To do this, we calculate the value of β_2, 100 times for 100 different statistically independent values of random phase difference γ, assumed to be uniformly distributed between $-\pi$ to $+\pi$. While calculating different values of β_2 for different values of γ, other parameters like S/N ratio, τ, and λ are kept constant.

3.5.1 Scheme to Estimate Normalized RMS Error

The r.m.s. value of β_2 for the pure measurement signal, $\beta_2 P_{rms}$ is given by,

$$\beta_2 P_{rms} = \left[\sum_{i=1}^{100} \beta_2 P_i^2 \, /100 \right]^{1/2} \qquad (3.11)$$

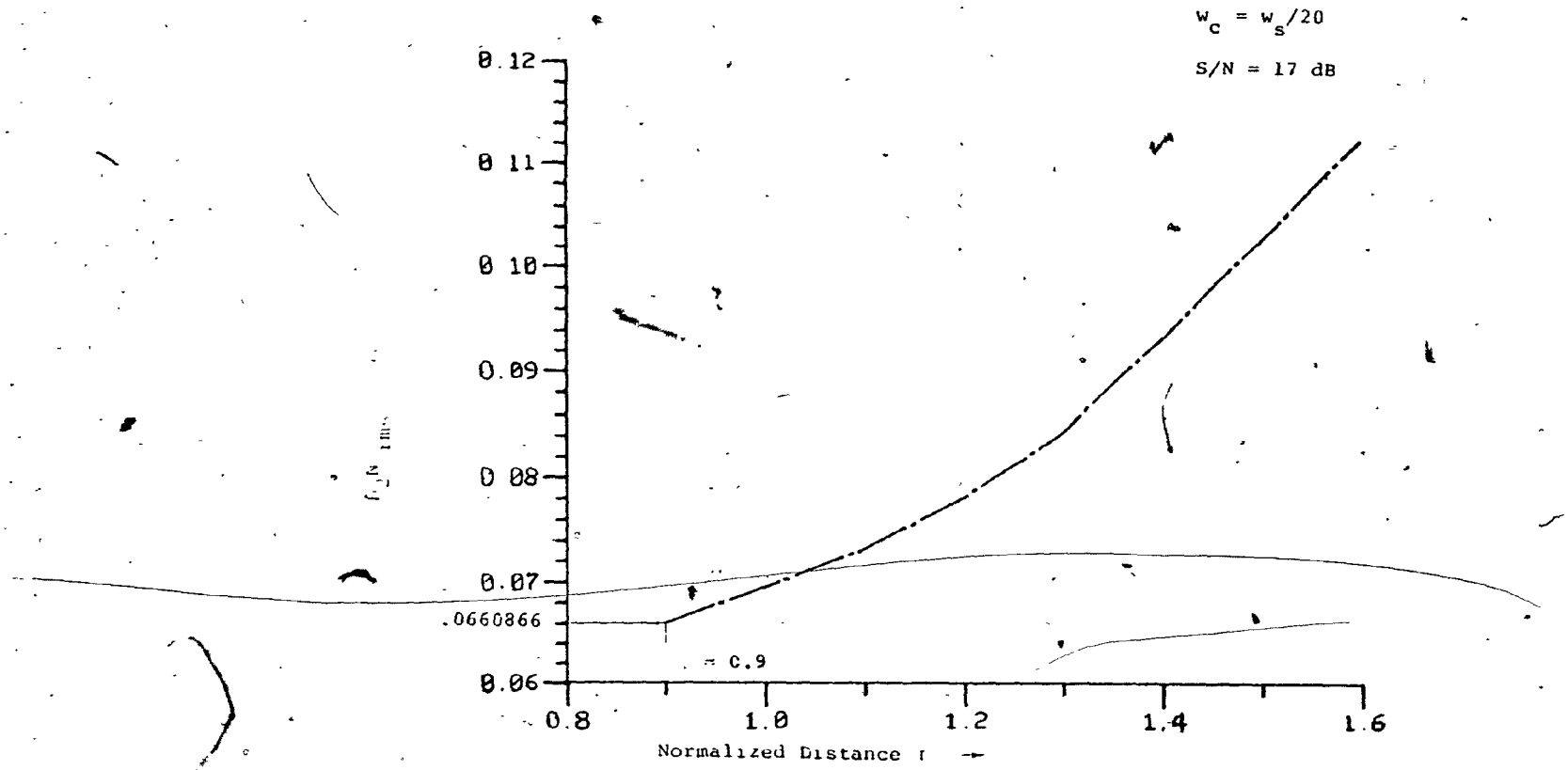

FIGURE 3.4: $P_2.N_{rms}$ vs r

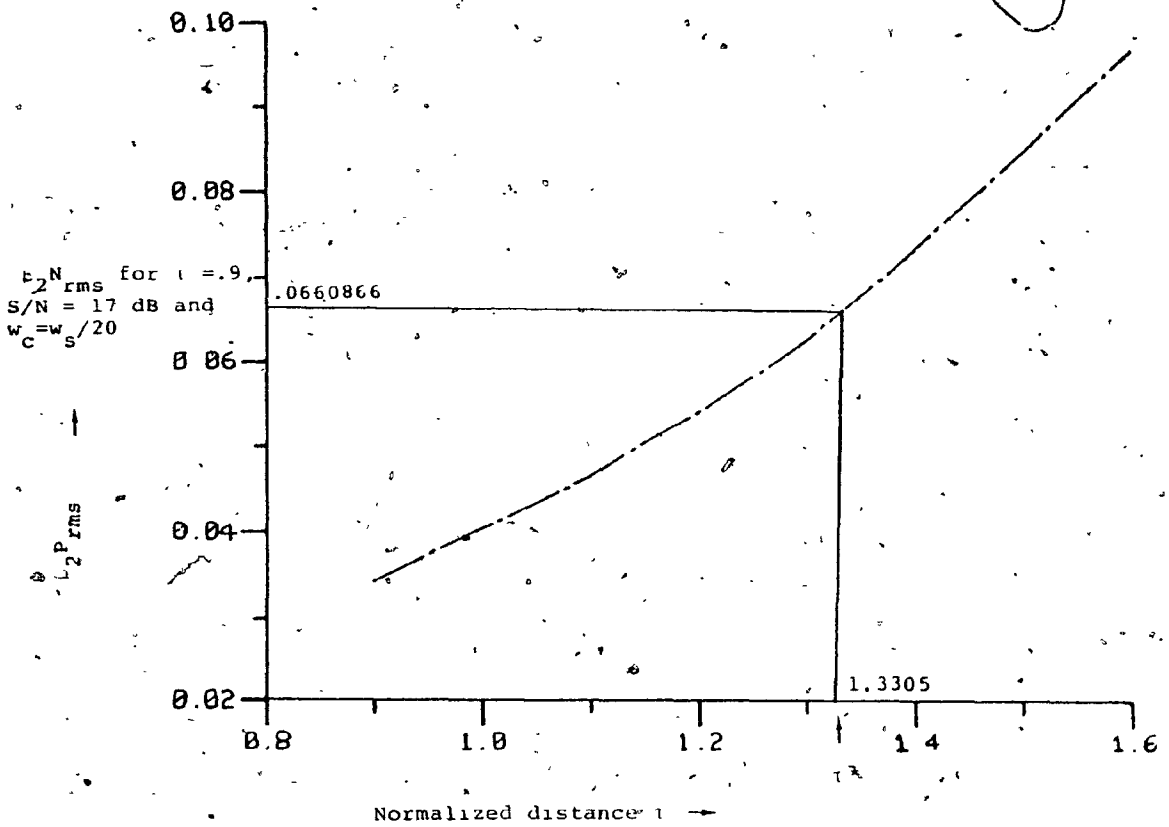

FIGURE 3.5: REFERENCE GRAPH

where $\beta_2 P_i$ are the β_2 values for the pure measurement signal.

Similarly, the r.m.s. value of β_2 for the noisy measurement signal, $\beta_2 N_{rms}$, is given by,

$$\beta_2 N_{rms} = \left[\sum_{i=1}^{100} \beta_2 N_i^2 / 100 \right]^{1/2} \qquad (3.12)$$

To estimate the r.m.s. error in determination of the normalized distance τ, two graphs are prepared. One graph between $\beta_2 N_{rms}$ and τ and the other one between $\beta_2 P_{rms}$ and τ as shown in Figures 3.4 and 3.5 are plotted. We call Figure 3.5 the reference graph. We change the value of τ in the computer simulation and record the corresponding value of β_{2rms}, in order to prepare the above graphs. Now to determine the r.m.s. error in measurement of a specific normalized distance, τ_1, for a fixed signal-to-noise ratio, and scattering strength α, we find out the corresponding value of $\beta_2 N_{rms}$ from Figure 3.4. By marking this value on the y axis of the reference graph and obtaining the corresponding value on the x-axis, we determine the estimated normalized distance, τ_1^*.

In the above procedure, we are transferring the r.m.s. value of $\beta_2 N_{rms}$ from the Y axis to the X axis to determine the r.m.s. value of τ^*. We justify our action by observing that the two curves have a similar shape and are almost linear.

Now the true error in distance measurement is equal to $\tau_1^* - \tau_1$, and the normalized r.m.s. error, ϵ, is equal to true error/pulse width, where the pulse width is equal to $2\sigma_p$.

TABLE 3.1

CALCULATION OF NORMALIZED R.M.S. ERROR ϵ

S/N ratio = 17dB, $w_c = w_s/20$, Equal RCS

τ	$\beta_2 P_{rms}$	$\beta_2 N_{rms}$	τ^*	$\epsilon = \frac{\tau^* - \tau}{2\sigma_p}$
0.9	0.0342448	0.0660866	1.3305	0.2152
1.0	0.0403303	0.0695926	1.3672	0.1836
1.1	0.0468383	0.0733949	1.3960	0.148
1.2	0.0542044	0.0782270	1.4440	0.122
1.3	0.0625275	0.0843516	1.50	0.10
1.4	0.0734289	0.0932483	1.57	0.085
1.5	0.0851121	0.1026498	--	--
1.6	0.0971880	0.1122440	--	--

TABLE 3.2

$w_c = w_s/20$, $\tau = 4/3$, EQUAL RCS

S/N ratio (dB)	$\beta_2 N_{rms}$	τ^*	$\epsilon = \frac{\tau^* - \tau}{2\sigma_p}$
10	0.124432	1.755	0.2108
12	0.1161779	1.713	0.1898
14	0.105534	1.6515	0.1590
16	0.092976	1.575	0.1208
18	0.080248	1.462	0.0645
20	0.068880	1.359	0.0128

Hence the normalized r.m.s. error is given by,

$$\epsilon = \frac{\tau^* - \tau}{2\sigma_p} \qquad (3.13)$$

Tables 3.1 and 3.2 show some actual values of parameters obtained during applying the algorithm and subsequently calculating ϵ.

3.5.2 Comparison of DF Algorithm Performance With Other Existing Algorithms

To compare the performance of the DF algorithm with the performance of the threshold and moment algorithms, we prepare two sets of curves showing normalized r.m.s. error against normalized distance τ and S/N ratio, while keeping other parameters fixed.

Figure 3.6 shows the normalized r.m.s. error vs normalized distance curves for all the three algorithms. Four different curves for the DF algorithm are shown for different cut off frequencies, w_c, of the digital filter, designed to correlate the noise for the received signal. In these figures w_s is the sampling angular frequency of the signal constructed.

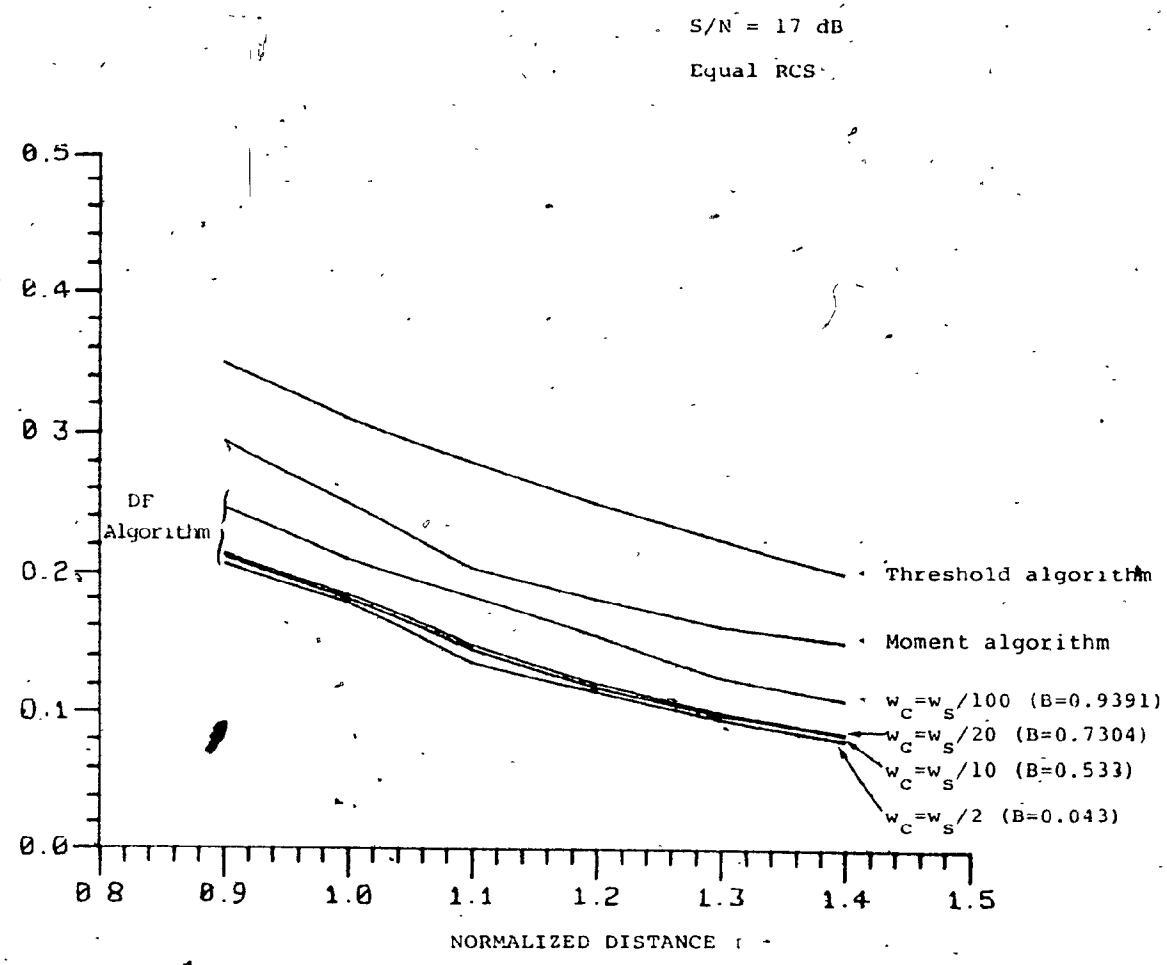

FIGURE 3.6: ERROR AS A FUNCTION OF DISTANCE

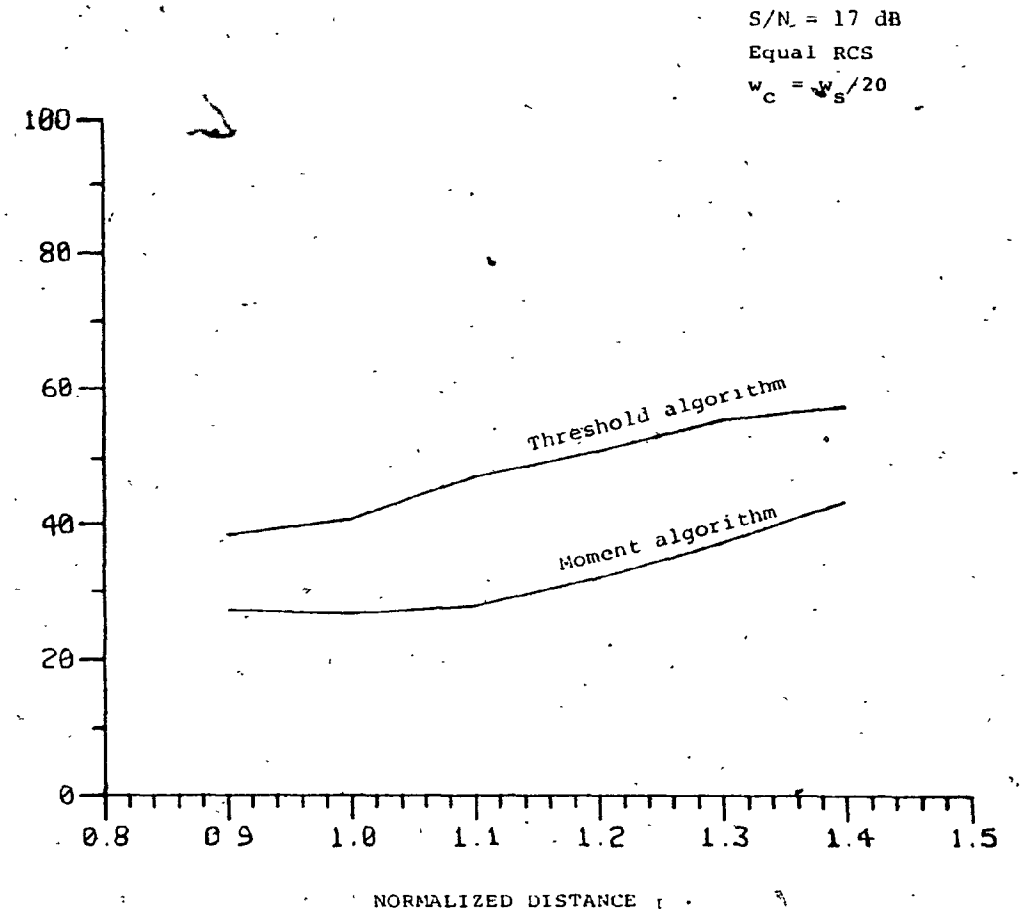

FIGURE 3.7: PERCENTAGE IMPROVEMENT BY DF ALGORITHM VS r

The signal-to-noise ratio is fixed to 17 dB and equal RCS is assumed. Cut-off frequencies equal to $w_{s/2}$, $w_{s/10}$, $w_{s/20}$ and $w_{s/100}$ are chosen for these curves. We observe that as the cut-off frequency of the filter is reduced, the bandwidth of the filter is reduced and the noise samples become more and more correlated. Consequently, the r.m.s. normalized error, ϵ is increased. Out of the four curves for the DF algorithm, the one with w_c equal to $w_{s/100}$, represents the maximum ϵ, but still is well below the performance curves corresponding to the moment and threshold algorithms [7]. Figure 3.7 shows the percentage improvement in the performance of the DF algorithm over the threshold and moment algorithms for a cut-off frequency equal to $w_{s/20}$ and a signal-to-noise ratio equal to 17 dB. It is observed from this figure, that the DF algorithm shows excellent performance improvement over the entire range of the normalized distance τ.

Figure 3.8 shows the variation of the normalized r.m.s. error versus the signal-to-noise ratio, while the normalized distance τ is kept constant, and equal to 4/3. The radar cross section for both point targets is again fixed to be equal. Here only two curves for the DF algorithm corresponding to cut-off frequencies of $w_{s/20}$ and $w_{s/100}$ are obtained, because these two are the cases, which produce maximum correlated noise. Here again the DF algorithm gives less normalized r.m.s. error ϵ in comparison to other algorithms, particularly for low and high S/N ratios. Figure 3.9 shows

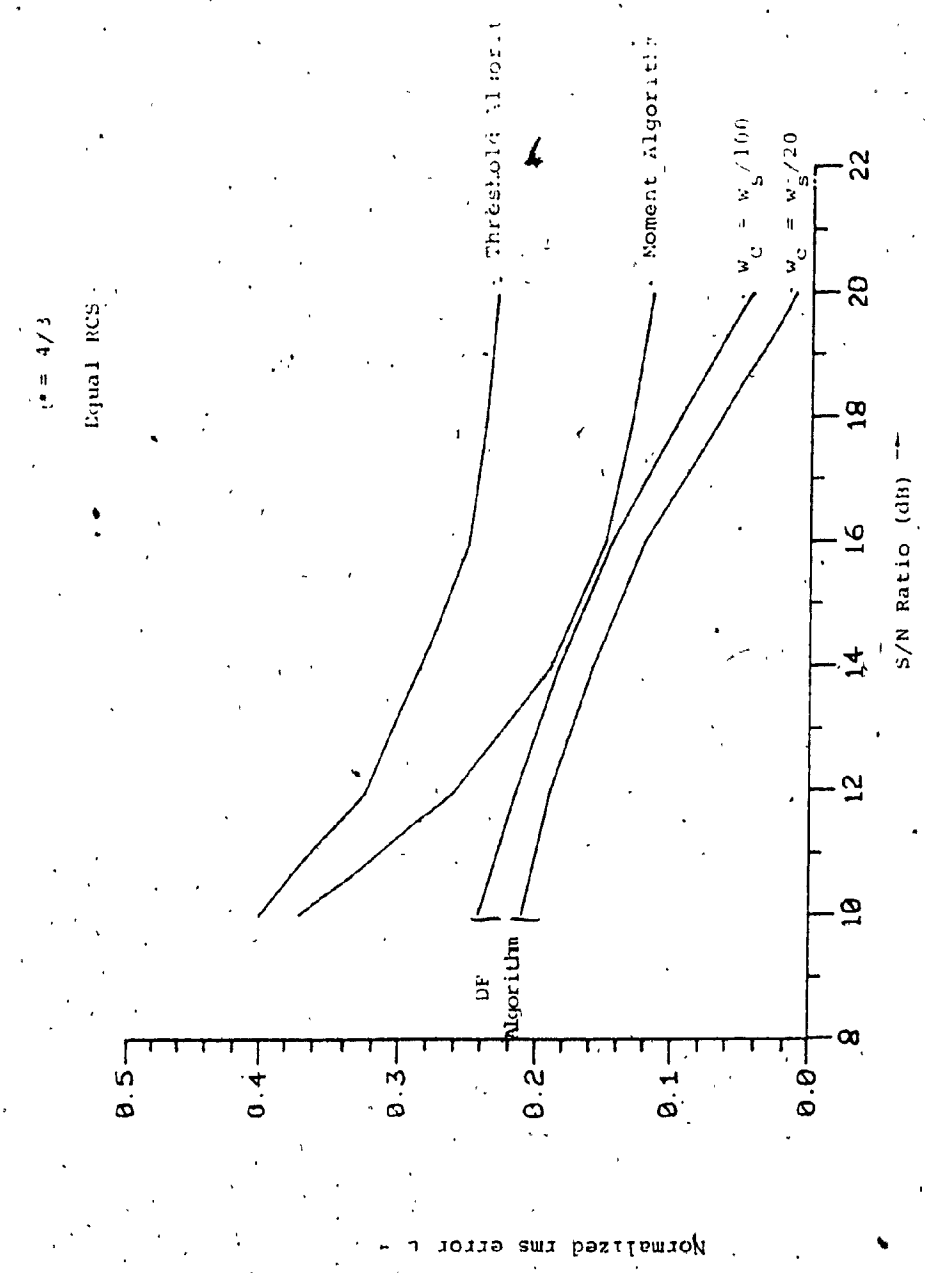

FIGURE 3.8: ERROR AS A FUNCTION OF S/N RATIO

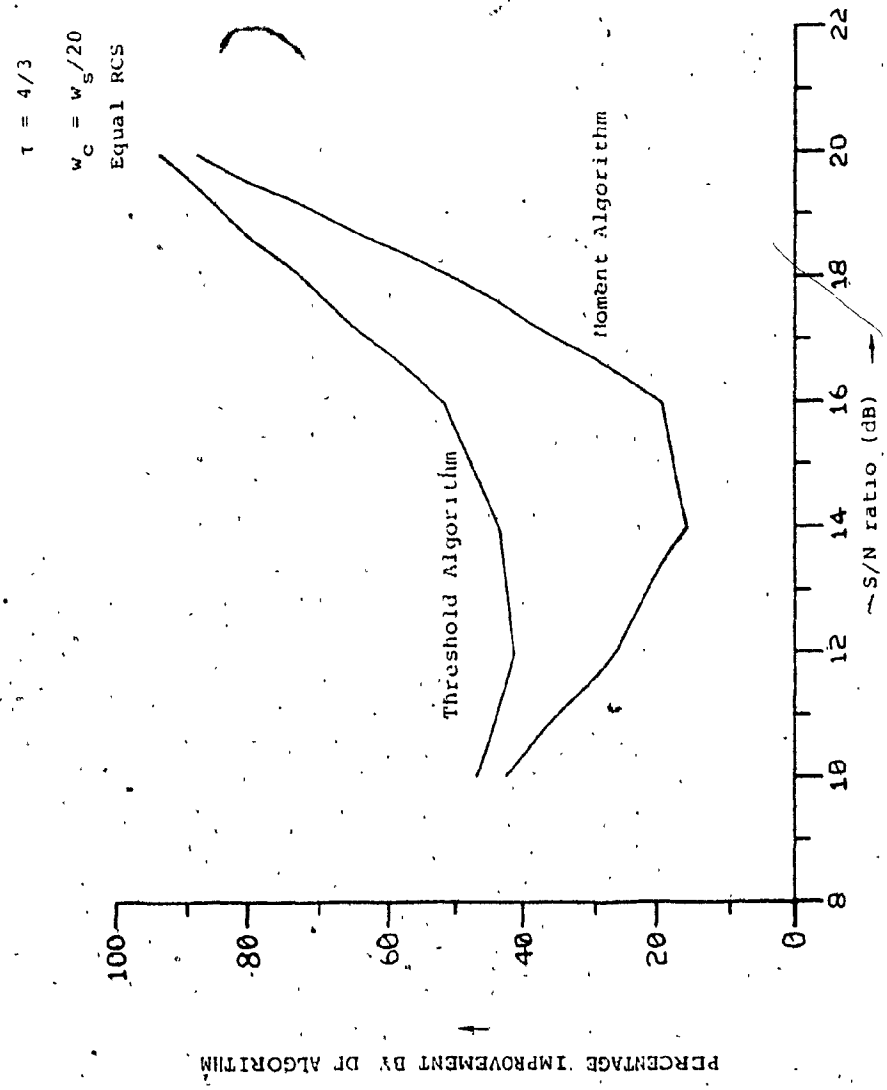

FIGURE 3.9: PERCENTAGE IMPROVEMENT BY DF ALGORITHM VS S/N RATIO

the percentage improvement of the DF algorithm over the threshold and moment algorithms, for w_c equal to $w_{s/20}$. It is noted that percentage improvement is smaller between S/N ratios of 12 and 16 dB, but increases rapidly for lower and higher values.

CHAPTER 4

CONCLUSIONS

Two main objectives have been achieved in this work:

(1) To provide an algorithm for detection of small differences in the shape of two signals, and

(2) To provide a new method for the measurement of the distance between two closely spaced point targets in radar systems.

In Chapter 2, the DF algorithm to detect small differences in the shape of two signals was described and illustrated with the help of several examples and figures. To implement the algorithm, two measurement signals, one combined (composite peak) and the other pure (single peak) were constructed. One pure reference signal was also constructed. Random noise, the level of which depends upon the desired signal-to-noise ratio, was added to the measurement signals. The distribution function of the measurement signals were calculated and compared with that of the reference signal, to obtain a function ϕ. The non-linearity of the function ϕ was estimated by applying the method of least-squares. The magnitude of this non-linearity designated by the parameter β_2, is proportional to the difference in the shapes of the measurement signal and the reference signal and proved to be a basis for detection of this difference. The algorithm was simulated on the computer and results were shown. The difference between two measurement signals, one combined and the other pure (both having a similar shape), was established for a S/N ratio of 25 dB. Some

general results in the form of curves were presented (Figure 2.9 to 2.12). These showed the variation of β_2 for different values of the ratios θ_2/θ_1 and σ_2/σ_1. The parameters θ_1, σ_1 and θ_2, σ_2 are the mean value and the standard deviation of component 1 and component 2, respectively, of the combined signal. The ratio θ_2/θ_1 ranged from 0.8798 to 1.12 and the ratio σ_2/σ_1 from 0.825 to 1.175. The values of these ratios were deliberately fixed to be quite near to unity. The idea behind this was to show that a distinction in the shapes can be made even when there is a very small deformation in the shape of the combined signal. On observing these curves it was found that for most of the range, the values of $|\beta_2|$ obtained in measuring the combined signal were significantly higher than those obtained for measuring the pure signal. As the ratios θ_2/θ_1 and σ_2/σ_1 deviated from unity, the magnitude of β_2 also increased, indicating more deformation in the shape of the combined signal. Also, we saw that in the case of the pure signal, a change of the ratio θ_2/θ_1 did not change the value of β_2. Finally, it can be remarked that if the deformation in the measurement signal was increased, detection was possible for lower signal-to-noise ratios.

As described in Chapter 3, the DF algorithm was used to provide a method for measuring the distance between two closely spaced point targets in radar systems. The incoming signals from the point targets were assumed to be of Gaussian

shape. Equal radar cross section of both the targets were assumed. The measurement noise was modelled as random noise having a Gaussian distribution with mean zero and standard deviation fixed according to a specified S/N ratio. The first return pulse from a single point target was used as the reference signal. The DF algorithm was applied and the value of β_2 calculated. This value of β_2 was then used to estimate the normalized distance τ between the point targets.

To judge the performance of the DF algorithm, the parameter β_2 was computed each time for 100 different values of the randomly received phase angle, γ, uniformly distributed between $-\pi$ and $+\pi$. Then the r.m.s. value of β_2 was calculated. A scheme to calculate the r.m.s. error made in the measurement of distance, was presented. For a signal-to-noise ratio equal to 17 dB and assuming equal RCS, the normalized r.m.s. errors made by the DF algorithm, corresponding to different normalized r.m.s. distance τ, were computed. These values were compared with the normalized r.m.s. errors obtained for the conventional threshold and moment algorithms. Four different curves (Figure 3.6) for the DF algorithm were presented corresponding to different cut-off frequencies w_c of a digital filter used to introduce input noise correlation. For w_c equal to $w_{s/100}$, where w_s is the angular sampling frequency, the noise samples were maximally correlated; the correlation coefficient B being equal to 0.9391. As shown, even for this case the normalized r.m.s. error made by the

DF algorithm was considerably less than that for the other algorithms. The percentage improvement in performance of the DF algorithm over the moment and threshold algorithms was computed and plotted for different normalized distances, for the cut off frequency of digital filter $w_c = w_s/20$. For τ equal to 0.9, the improvement over the threshold and the moment algorithms was found to be 38% and 27%, respectively, improving to 57% and 43% respectively, for τ equal to 1.4 (Figure 3.7). To see the variation of the normalized r.m.s. error $\in$ for different S/N ratios, τ was kept constant and equal to 4/3. Again equal RCS were assumed and the normalized r.m.s. error made for the DF algorithm was computed and compared with the other algorithms (Figures 3.8 and 3.9). As observed from Figure 3.9, the percentage improvement in the performance of the DF algorithm was lower for S/N ratios between 12 dB and 16 dB, but increased steeply for higher and lower values of the S/N ratio. For a S/N ratio of 20 dB, the precentage improvement of the DF algorithm over the threshold and the moment algorithm was seen to be 94% and 88%, respectively.

In conclusion, it can be said that the DF algorithm provides some useful and interesting results in the field of signal detection and classification, and is able to reduce the error in radar measurements. Still there may be other applications as suggested in Chapter 1, where this algorithm can be fruitfully employed. Future work may be suggested in

the form of hardware implementation of the DF algorithm. An independent hardware unit using a microprocessor may be designed, which can perform the basic and simple calculations required for this algorithm.

APPENDIX 1

DETERMINATION OF STANDARD DEVIATION OF WHITE NOISE FOR A FIXED S/N RATIO

As shown in the figure, we assume a combined signal made of two Gaussian components, the normalized distance between them being equal to τ_o.

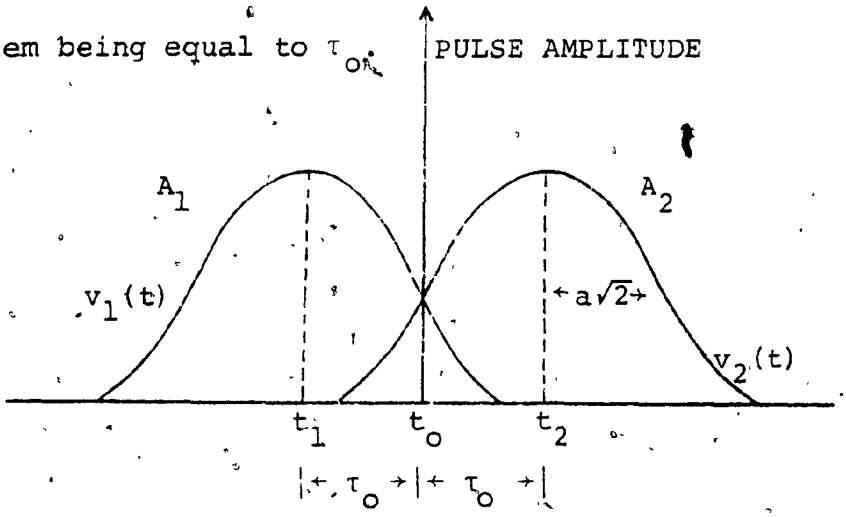

FIGURE A1.1: Combined Signal (Adding Two Gaussian Components)

Let A_1 = Amplitude of the first component,

A_2 = Amplitude of the second component,

and, $a\sqrt{2}$ = Standard deviation of any component.

The first component is,

$$v_1(t) = A_1 \exp(+j\gamma/2) \exp\left\{\left(-\frac{1}{4a^2}\right)[t-(t_o-\tau_o)]^2\right\} \qquad \text{(A1-1)}$$

The second component is,

$$v_2(t) = A_2 \exp(-j\frac{\gamma}{2}) \exp\left\{\left(-\frac{1}{4a^2}\right)[t-(t_o+\tau_o)]^2\right\} \qquad \text{(A1-2)}$$

where γ = Radio frequency (RF) phase between individual pulses uniformly distributed between $-\pi$ to $+\pi$.

The complex video signal would be,

$$v(t) = v_1(t) + v_2(t)$$

The received pulse is then given by [8],

$$|v(t)|^2 = A_1^2 \exp\{(-\frac{1}{2a^2})[t-(t_o-\tau_o)]^2\} + A_2^2 \exp\{(-\frac{1}{2a^2})[t-(t_o+\tau_o)]^2\} + 2A_1A_2 \cos\gamma \exp\{(-\frac{1}{2a^2})[(t-t_o)^2+\tau_o^2]\} \quad (A1-3)$$

Let m_o = Signal energy over time T.

$m_o = \mu_o$

where μ_o is the oth non central moment of $|v(t)^2|$.

Hence, we obtain [9],

$$m_o = a\sqrt{2\pi}\ [A_1^2+A_2^2+2A_1A_2 \exp(-\tau_o^2/2a^2)\cos\gamma] \quad (A1-4)$$

The Expected value of m_o (averaging over γ), from (A1-4) is,

$$\bar{m}_o = E\{m_o\} \simeq a\sqrt{2\pi}\ [A_1^2 + A_2^2] \quad (A1-5)$$

Let the standard deviation of the white noise equal σ_n; then the average signal energy-to-noise power ratio [9] is,

$$\delta av = \frac{\bar{m}_o}{2\sigma_n^2} \text{ in dB} \quad (A1-6)$$

Expressing (A1-6) in decibels we have,

$$\delta av. \text{ in dB} = 10 \cdot \log_{10}\left[\frac{\bar{m}_o}{2\sigma_n^2}\right] \quad (A1-7)$$

Solving (A1-7) for the standard deviation of the noise, we obtain,

$$\sigma_n = \sqrt{\frac{\bar{m}_o}{2x10^{\delta av/10}}} \quad (A1-8)$$

APPENDIX 2

ESTIMATION OF THE PARAMETER β_2

We have the data points for $\phi(x)$,

$\{x_i\}$ for $i = 1,2,....,n$ (On the x-axis)

$\{y_i\}$ for $i = 1,2,....,n$ (On the y-axis)

We apply the METHOD OF LEAST SQUARES to fit the curve to above data. Using the parabolic equation,

$$y = \beta_o + \beta_1 x + \beta_2 x^2 , \qquad \text{(A2-1)}$$

we can estimate the coefficients β_o, β_1 and β_2. Here we are interested in estimating, only β_2.

Let the estimated values of β_o, β_1 and β_2 in (A2-1) be $\hat{\beta}_o$, $\hat{\beta}_1$, and $\hat{\beta}_2$, and we will fit the parabola,

$$\hat{y} = \hat{\beta}_o + \hat{\beta}_1 x + \hat{\beta}_2 x^2 \qquad \text{(A2-2)}$$

to a set of paired data $\{(x_i,y_i)\ i = 1,2,....,n\}$.

Let

$$Q = \sum_{i=1}^{n} [y_i - (\hat{\beta}_o + \hat{\beta}_1 x_i + \hat{\beta}_2 x_i^2)] \qquad \text{(A2-3)}$$

Minimizing Q yields the following set of equations [6],

$$\sum_{i=1}^{n} y_i = \hat{\beta}_o n + \hat{\beta}_1 \sum_{i=1}^{n} x_i + \hat{\beta}_2 \sum_{i=1}^{n} x_i^2 \qquad \text{(A2-4)}$$

$$\sum_{i=1}^{n} x_i y_i = \hat{\beta}_o \sum_{i=1}^{n} x_i + \hat{\beta}_1 \sum_{i=1}^{n} x_i^2 + \hat{\beta}_2 \sum_{i=1}^{n} x_i^3 \qquad \text{(A2-5)}$$

$$\sum_{i=1}^{n} x_i^2 y_i = \hat{\beta}_o \sum_{i=1}^{n} x_i^2 + \hat{\beta}_1 \sum_{i=1}^{n} x_i^3 + \hat{\beta}_2 \sum_{i=1}^{n} x_i^4 \qquad \text{(A2-6)}$$

To simplify the above expressions and further calculations, let

$$\sum_{i=1}^{n} x_i = A_1$$

$$\sum_{i=1}^{n} x_i^2 = A_2$$

$$\sum_{i=1}^{n} x_i^3 = A_3$$

$$\sum_{i=1}^{n} x_i^4 = A_4$$

$$\sum_{i=1}^{n} y_i = C_1$$

$$\sum_{i=1}^{n} x_i y_i = C_2$$

$$\sum_{i=1}^{n} x_i^2 y_i = C_3$$

By substituting these in equations (A2-4), (A2-5), and (A2-6), we obtain,

$$C_1 = \hat{\beta}_o n + \hat{\beta}_1 A_1 + \hat{\beta}_2 A_2 \qquad \text{(A2-4)}$$

$$C_2 = \hat{\beta}_o A_1 + \hat{\beta}_1 A_2 + \hat{\beta}_2 A_3 \qquad \text{(A2-5)}$$

$$C_3 = \hat{\beta}_o A_2 + \hat{\beta}_1 A_3 + \hat{\beta}_2 A_4 \qquad \text{(A2-6)}$$

From equation (A2-4),

$$\hat{\beta}_o = \frac{(C_1 - \hat{\beta}_1 A_1 - \hat{\beta}_2 A_2)}{n}$$

Substituting $\hat{\beta}_o$ in equation (A2-5),

$$C_2 = \left(\frac{C_1 - \hat{\beta}_1 A_1 - \hat{\beta}_2 A_2}{n}\right) A_1 + \hat{\beta}_1 A_2 + \hat{\beta}_2 A_3$$

$$nC_2 = C_1 A_1 - \hat{\beta}_1 A_1^2 - \hat{\beta}_2 A_1 A_2 + n\hat{\beta}_1 A_2 + n\hat{\beta}_2 A_3 \qquad \text{(A2-7)}$$

Substituting $\hat{\beta}_o$ in equation (A2-6),

$$C_3 = \left(\frac{C_1 - \hat{\beta}_1 A_1 - \hat{\beta}_2 A_2}{n}\right) A_2 + \hat{\beta}_1 A_3 + \hat{\beta}_2 A_4$$

or $$nC_3 = C_1 A_2 - \hat{\beta}_1 A_1 A_2 - \hat{\beta}_2 A_2^2 + n\hat{\beta}_1 A_3 + n\hat{\beta}_2 A_4 \qquad \text{(A2-8)}$$

From equation (A2-7),

$$nC_2 - C_1 A_1 + \hat{\beta}_2 A_1 A_2 - n\hat{\beta}_2 A_3 = \hat{\beta}_1 (nA_2 - A_1^2)$$

$$\hat{\beta}_1 = \frac{nC_2 - C_1 A_1 + \hat{\beta}_2 A_1 A_2 - n\hat{\beta}_2 A_3}{nA_2 - A_1^2}$$

Substituting the value of $\hat{\beta}_1$ in equation (A2-8),

$$nC_3 = C_1A_2 - \hat{\beta}_2A_2^2 + n\hat{\beta}_2A_4 + (nA_3 - A_1A_2)$$

$$\times \frac{nC_2 - C_1A_1 + \hat{\beta}_2A_1A_2 - n\hat{\beta}_2A_3}{nA_2 - A_1^2}$$

$$nC_3(nA_2-A_1^2) = (nA_2-A_1^2)(C_1A_2 - \hat{\beta}_2A_2^2 + n\hat{\beta}_2A_4)$$

$$+ (nA_3-A_1A_2)(nC_2 - C_1A_1 + \hat{\beta}_2A_1A_2 - n\hat{\beta}_2A_3)$$

or $$nC_1A_2^2 - n\hat{\beta}_2A_2^3 + n^2\hat{\beta}_2A_2A_4 - C_1A_1^2A_2 + \hat{\beta}_2A_1^2A_2^2$$

$$-n\hat{\beta}_2A_1^2A_4 + n^2A_3C_2 - nA_1C_1A_3 + n\hat{\beta}_2A_1A_2A_3$$

$$-n^2\hat{\beta}_2A_3^2 - nA_1A_2C_2 + C_1A_1^2A_2 - \hat{\beta}_2A_1^2A_2^2$$

$$+n\hat{\beta}_2A_1A_2A_3 = nC_3(nA_2-A_1^2)$$

$$\hat{\beta}_2 = \frac{[nC_3(nA_2-A_1^2)-nC_1A_2^2-n^2A_3C_2+nA_1C_1A_3 + nA_1A_2C_2]}{[n^2A_2A_4-nA_2^3-nA_1^2A_4+2nA_1A_2A_3-n^2A_3^2}$$

or $$\hat{\beta}_2 = \frac{n[C_3(nA_2-A_1^2)+C_1(A_1A_3-A_2^2)-nA_3C_2 + A_1A_2C_2]}{n[A_4(nA_2-A_1^2)-nA_3^2+2A_1A_2A_3-A_2^3]} \qquad \text{(A2-9)}$$

APPENDIX 3

1. DESIGN OF FIRST ORDER, RECURSIVE, LOWPASS DIGITAL FILTER

To design a first order, recursive, lowpass digital filter, a Butterworth analog filter approximation is obtained [10]. The complete design procedure is carried out in three major steps. This approach is simpler and more direct than the approach of Baum [7], as described in [11].

1.A. THE NORMALIZED LOWPASS TRANSFER FUNCTION

The normalized transfer function is given by,

$$H_N(s) = \frac{1}{\prod_{i=1}^{n} (s-p_i)} \qquad \text{(A3-1)}$$

where n is the order of the filter and p_i for i=1,2,....,n are the left half s-plane zeros of the loss function $L(-s^2)$.

Since,

$$L(-s^2) = \prod_{k=1}^{2n} (s-s_k)$$

where

$$s_k = \begin{cases} e^{j(2k-1)\pi/2n} & \text{for even } n \\ e^{j(k-1)\pi/n} & \text{for odd } n \end{cases} \qquad \text{(A3-2)}$$

Substituting n = 1 in (A3-2) and trying to get left half s plane zeros we proceed as follows:

For k = 1,

$$s_1 = \cos 0 + j \sin 0$$

$$s_1 = 1$$

This is positive, so the zero is in the right half s-plane. We reject it, and for k = 2,

$$s_2 = \cos \pi + j \sin \pi$$

$$s_2 = -1$$

So the normalized transfer function is,

$$H_N(s) = \frac{1}{s+1} \qquad \text{(A3-3)}$$

1.B. THE UNNORMALIZED LOWPASS TRANSFER FUNCTION

The unnormalized low pass transfer function can easily be obtained by using the transformation,

$$s = \lambda \bar{s}$$

as $s = jw$, and $\bar{s} = j\bar{w}$

we have,

$$w = \lambda \bar{w}$$

For the normalized transfer function we have, w = 1 rad/sec. Let $\bar{w}$ be the desired cut-off frequency of the digital filter and designate it by w_c.

Then,

$$\lambda = \frac{1}{w_c}$$

Hence, the unnormalized transfer function is,

$$H_A(\bar{s}) = \frac{1}{\lambda \bar{s}+1}$$

$$= \frac{1}{\bar{s}/w_c+1}$$

or, $$H_A(\bar{s}) = \frac{w_c}{\bar{s}+w_c} \qquad \text{(A3-4)}$$

1.C. THE RECURSIVE DIGITAL FILTER TRANSFER FUNCTION

A recursive filter approximation can be obtained from the preceding analog filter approximations using the Invariant Impulse response method.

The Impulse response of the analog filter is,

$$h_A(t) = L^{-1}\{H_A(\bar{s})\}$$

where $L^{-1}\{H_A(\bar{s})\}$ is the Inverse Laplace transform of $H_A(\bar{s})$. From (A3-4), we obtain,

$$h_A(t) = L^{-1}\left\{\left[\frac{w_c}{\bar{s}+w_c}\right]\right\}$$

or, $$h_A(t) = w_c\, e^{-w_c t}$$

Let T be the sampling period, and replacing t by nT, we have,

$$h_A(nT) = w_c\, e^{-w_c nT}$$

Taking the Z-transform of $h_A(nT)$, we obtain the transfer function of the digital filter $H_D(z)$, i.e.,

$$H_D(z) = Z\{h_A(nT)\} = Z\{w_c\, e^{-w_c nT}\}$$

$$H_D(z) = \frac{w_c z}{z - e^{-w_c T}} \qquad \text{(A3-5)}$$

2. DETERMINATION OF THE MULTIPLYING FACTORS "A" AND "B" IN THE AUTOREGRESSION EQUATION

A first order autoregression equation can be written as,

$$y_{n+1} = B\, y_n + A\, x_{n+1} \qquad \text{(A3-6)}$$

where x_n represents input samples and y_n are the output correlated samples. The coefficients A and B are the multiplying factors.

Here we formulate the expressions for A and B by comparing the transfer function of the first order autoregression model to the transfer function of the first order digital filter.

Taking the Z-transform of equation (A3-6), we have

$$ZY(z) = BY(z) + Az\, x(z)$$

$$Y(z)\ (z-B) = Az\, x(z)$$

or,

$$H(z) = \frac{Y(z)}{x(z)} = \frac{Az}{z-B}$$

Thus, the transfer function H(z) is equal to,

$$H(z) = \frac{Az}{z-B} \qquad \text{(A3-7)}$$

Comparing equation (A3-5) to (A3-7), we obtain,

$$A = w_c$$

and, $$B = e^{-w_c T} \qquad \text{(A3-8)}$$

where w_c is the cut-off frequency of the digital filter in rad/sec.

APPENDIX 4

COMPUTER PROGRAM USED FOR CHAPTER 2

```
      PROGRAM GARG(INPUT,OUTPUT,TAPE1,TAPE2,TAPE3,TAPE4,TAPE7,
     +TAPE8)
      REAL VP(1800),S(1800),VDF(1800),SDF(1800),XA(1800),NOISEP
      REAL X(30),Y(30),AT(1800),A(30),DF(1800),NUM,LOGA,LNA
      REAL NOISEC,NV(1800),VNF(1800),VPF(1800),SNR,DEV(30)
      REAL VP(1800),THETAR(11)
      REAL PVN(1800),PVF(1800),VV(1800,2),BETAX(11,5)
      DIMENSION IMAG4(5151),ITITLE(144),ICHAR(10),RANGE(4)
      DATA ICHAR(1)/1H /,RANGE/4*0.0/
      ITITLE(1)=0
      PI=3.14159
      SNR=40.
82    SIGMA1=0.4
      THETA1=2.08
      PRINT 100,THETA1,SIGMA1
100   FORMAT(5X,"** REFERENCE SIGNAL HAS MEAN=",F4.2," & STANDARD
     + DEVIATION=",F4.2," **",//)
      PRINT 101,THETA1,SIGMA1
101   FORMAT(///,5X,"** COMPONENT #1 OF MIXED SIGNAL HAS MEAN=",
     +F4.2," & STANDARD DEVIATION=",F4.2," **")
      DO 1 II=1,5
      SIGMA2=.295+.035*II
      PRINT 102,SIGMA2
102   FORMAT(//,5X," COMPONENT #2 OF MIXED SIGNAL HAS S.D.=",F5.3
     +," **",//)
      PRINT 104
104   FORMAT(1X,"* MEAN OF COMPONENT #2*",3X,"* MEAN OF PURE SIGNAL *
     +",4X,"S.D.OF PURE SIGNAL *",4X,"BETA0",9X,"BETA1",7X,"BETA2")
      DO 2 III=1,11
      THETA2=1.73+III*0.05
      SD=0.0
      VD=0.0
      VPP=0.0
      N=1800
      VMAX1=0.0
      VMAX2=0.0

C     * CONSTRUCTING THE COMPONENTS OF THE COMBINED MEASUREMENT SIGNAL*
      DO 10 I=1,N
      T=FLOAT(I)/420.
      XA(I)=T
      VV(I,1)=EXP(-(T-THETA1)**2/(2*SIGMA1**2))/(SQRT(2.*PI)*SIGMA1)
      VV(I,2)=EXP(-(T-THETA2)**2/(2*SIGMA2**2))/(SQRT(2.*PI)*SIGMA2)
      IF(VMAX1.LT.VV(I,1))  VMAX1=VV(I,1)
      IF(VMAX2.LT.VV(I,2))  VMAX2=VV(I,2)
10    CONTINUE
```

```
C   ** CALCULATION OF PROPORTIONALITY FACTOR (ALPHA) **
      VMAX=VMAX1+VMAX2
      ALPHA=VMAX1/VMAX

12    FORMAT(2X,"VMAX1=",F8.6,3X,"VMAX2=",F8.6,3X,"ALPHA=",F5.3)
      XM=ALPHA*THETA1+(1-ALPHA)*THETA2
      M1=THETA1-XM
      M2=THETA2-XM
      VAR2=ALPHA*(SIGMA1**2+M1**2)+(1-ALPHA)*(SIGMA2**2+M2**2)
      STD2=SQRT(VAR2)
      VMAXP=0.0
      DO 11 I=1,N
      T=FLOAT(I)/420.
      VT(I)=ALPHA*VV(I,1)+(1-ALPHA)*VV(I,2)
      VP(I)=EXP(-(T-XM)**2/(2*STD2**2))/(SQRT(2.*PI)*STD2)
      IF (VMAXP.LT.VP(I))  VMAXP=VP(I)
      VO=VO+VT(I)
      SO=SO+VV(I,1)
      VPP=VPP+VP(I)
      VOF(I)=VO
      SOF(I)=SO
      VPF(I)=VPP
11    CONTINUE

C   ** CALCULATION OF STANDARD DEVIATION OF NOISE **
      POWERC=STD2*SQRT(PI)*(VMAX1**2+VMAX2**2)
      POWERP=STD2*SQRT(PI)*VMAXP**2
      SDNC=SQRT(POWERC/(2.*EXP(2.3025851*SNR/10.)))
      SDNP=SQRT(POWERP/(2.*EXP(2.3025851*SNR/10.)))
      VN=0.0
      PN=0.0

C   ** CONSTRUCTING THE NOISY MEASUREMENT SIGNAL **
      DO 15 I=1,N
      AA=RANF(1)
      NOISEC=(AA-0.5)*SQRT(12.)*SDNC
      NOISEP=(AA-0.5)*SQRT(12.)*SDNP
      VT(I)=VT(I)+NOISEC
      VP(I)=VP(I)+NOISEP
      VN=VN+VT(I)
      VNF(I)=VN
      PN=PN+VP(I)
      PVF(I)=PN
15    CONTINUE

      DO 20 I=1,N
      NV(I)=VNF(I)/VNF(N)
```

```
      S(I)=SDF(I)/SDF(N)
      PVN(I)=PVF(I)/PVF(1800)
20    CONTINUE

C  ** COMPARING THE D.F. OF THE MEASUREMENT SIGNAL TO THE REFERENCE
 C       SIGNAL **
      DO 30 J=1,2
      KK=1
      XX=0.04
      IF (J.EQ.2) GO TO 45
      DO 61  I=1,N
      DF(I)=S(I)
61    AT(I)=XA(I)
      GO TO 46
45    DO 62 I=1,N
      DF(I)=PVN(I)
62    AT(I)=XA(I)
46    DO 40 K=1,35
      DO 52 I=1,N
      X1=XX-.009
      X2=XX+.009
      IF (DF(I).LE.X2.AND.DF(I).GE.X1) GO TO 51
      GO TO 52
51    DEVMIN=0.1
      DO 56 I1=1,30
56    DEV(I1)=ABS(DF(I+I1-1)-XX)
      DO 57 I2=1,30
      IF(DEV(I2).GT.DEVMIN) GO TO 57
      DEVMIN=DEV(I2)
      I3=I+I2-1
57    CONTINUE
      A(KK)=AT(I3)
      IF (J.EQ.1)  X(KK)=A(KK)
      IF (J.EQ.2)  Y(KK)=A(KK)
      GO TO 17
52    CONTINUE
      M=KK-1
      IF (J.EQ.1) GO TO 30
      IF (J.EQ.2) GO TO 14
17    KK=KK+1
      XX=XX+.035
40    CONTINUE
30    CONTINUE

C-  ** ESTIMATING THE PARAMETER BETA2 **
14    A1=0.0
      A2=0.0
```

```
      A3=0.0
      A4=0.0
      C1=0.0
      C2=0.0
      C3=0.0
      DO 70 I=1,M
      A1=X(I)+A1
      A2=X(I)**2+A2
      A3=X(I)**3+A3
      A4=X(I)**4+A4
      C1=Y(I)+C1
      C2=X(I)*Y(I)+C2
      C3=X(I)**2*Y(I)+C3
70    CONTINUE
      NUM=M*(C3*(M*A2-A1**2)+C1*(A1*A3-A2**2)-M*A3*C2+A1*A2*C2)
      DEN=M*(A4*(M*A2-A1**2)-M*A3**2+2.*A1*A2*A3-A2**3)
      BETA2=NUM/DEN
      PRINT 105,THETA2,XM,STD2,BETA2
105   FORMAT(3X,F4.2,23X,F4.2,23X,F4.2,13X,E12.6,/)
      BETAX(III,II)=BETA2
      THETAR(III)=THETA2/THETA1
      IF (II.EQ.1)  PRINT (3,*) THETAR(III)
      IF (II.EQ.1)  PRINT (1,*) BETAX(III,1)
      IF (II.EQ.2)  PRINT (2,*) BETAX(III,2)
      IF (II.EQ.3)  PRINT (3,*)  BETAX(III,3)
      IF (II.EQ.4)  PRINT (4,*)  BETAX(III,4)
      IF (II.EQ.5)  PRINT (7,*)  BETAX(III,5)
2     CONTINUE
      PRINT 12,VMAX1,VMAX2,ALPHA
1     CONTINUE
      CALL USPLT(THETAR,BETAX,11,11,5,1,TITLE,RANGE,ICHAR,1,IMAG
     +4',IER)
      STOP
      END
```

COMPUTER PROGRAM USED FOR CHAPTER 3

```
      PROGRAM GARG(INPUT,OUTPUT,TAPE5,TAPE6)
      REAL VT(1800),ST(1800),S(1800),VDF(1800),SDF(1800)
      REAL X(30),Y(30),AT(1800),A(30),DF(1800),NUM,VV(1800,2)
      REAL VTN(1800),NV(1800),DEV(40),VTF(1800),NR(1800),XA(1800)
      REAL IMAG,IMAGN,V(1800),YR2(1800),YI2(1800),NI(1800)
      DOUBLE PRECISION DSEED1,DSEED2
      DSEED2=12389.D0
      DSEED1=554798.D0
      PI=3.14159
      SNR=20.
      N=1800
      SIGMAP=1.0
      THETA2=1.9
      TAO2=THETA2/SIGMAP
      THETA1=-1.9
      TAO1=THETA1/SIGMAP
      ALPHA=0.5
      VMAX=0.0

C     ** CONSTRUCTING THE EACH TARGET RESPONSE SEPARATELY **
      DO 10 I=1,N
      T=FLOAT(I-N/2)/220.
      XA(I)=T
      VV(I,1)=EXP(-(T-TAO1)**2/(2*SIGMAP**2))/(SQRT(2.*PI)*SIGMAP)
      VV(I,2)=EXP(-(T-TAO2)**2/(2*SIGMAP**2))/(SQRT(2.*PI)*SIGMAP)
      IF(VMAX.LT.VV(I,1))  VMAX=VV(I,1)
10    CONTINUE

C     *CALCULATING THE STANDARD DEVIATION OF ADDITIVE WHITE NOISE*
      POWERS=SIGMAP*SQRT(PI)*2.*VMAX**2
      SDN=SQRT(POWERS/(2.*EXP(2.3025851*SNR/10.)))

      BETAT=0.0

C     ** CALCULATION OF BETA2 FOR 100 DIFFERENT VALUES OF PHASE ANGLE **
      DO 2 III=1,100
      SD=0.0
      VD=0.0
      VTT=0.0
      PHD=(RANF(1)-0.5)*PI
      TT=1./220.
      WC=PI/(TT*50)
      AA=WC
      B=EXP(-AA/220.)
      YR2T=0.0
      YI2T=0.0
      YR2S=0.0
```

```
      YI2S=0.0
      Y1=0.0
      Y2=0.0

C  ** CORRELATING THE WHITE NOISE ACCORDING TO THE CUTOFF
C     FREQUENCY OF THE DIGITAL FILTER **
      DO 21 K1=1,N
      YR2(K1)=AA*GGNQF(DSEED1)+B*Y1
      YI2(K1)=AA*GGNQF(DSEED2)+B*Y2
      Y1=YR2(K1)
      Y2=YI2(K1)
      YR2T=YR2T+YR2(K1)
      YI2T=YI2T+YI2(K1)
21    CONTINUE
      YR2M=YR2T/N
      YI2M=YI2T/N
      DO 22 K2=1,N
      YR2S=YR2S+(YR2(K2)-YR2M)**2
      YI2S=YI2S+(YI2(K2)-YI2M)**2
22    CONTINUE
      STDR=SQRT(YR2S/N)
      STDI=SQRT(YI2S/N)
      DO 12 K1=1,N
      NR(K1)=(YR2(K1)-YR2M)*SDN/STDR
      NI(K1)=(YI2(K1)-YI2M)*SDN/STDI
12    CONTINUE

C  ** ADDING THE NOISE TO MEASURED TWO TARGET RESPONSE **
      DO 11 I=1,N
      T=FLOAT(I-N/2)/220.
      REAL=COS(PHD)*(ALPHA*VV(I,1)+(1-ALPHA)*VV(I,2))
      IMAG=SIN(PHD)*(ALPHA*VV(I,1)-(1-ALPHA)*VV(I,2))
      VT(I)=SQRT(REAL**2+IMAG**2)
      REALN=REAL+NR(I)
      IMAGN=IMAG+NI(I)
      VTN(I)=SQRT(REALN**2+IMAGN**2)

C  * REFERENCE SIGNAL CONSTRUCTED AS THE FIRST TARGET RESPONSE *
      ST(I)=VV(I,1)

      VD=VD+VT(I)
      SD=SD+ST(I)
      VTT=VTT+VTN(I)
      VDF(I)=VD
      SDF(I)=SD
      VTF(I)=VTT
11    CONTINUE
```

```
      DO 20 I=1,N
      V(I)=VDF(I)/VDF(N)
      NV(I)=VTF(I)/VTF(N)
      S(I)=SDF(I)/SDF(N)
20    CONTINUE
C   ** COMPARING THE DISTRIBUTION FUNCTIONS **

      DO 30 J=1,2
      KK=1
      XX=0.04
      IF (J.EQ.2) GO TO 45
      DO 61  I=1,N
      DF(I)=S(I)
61    AT(I)=XA(I)
      GO TO 46
45    DO 62 I=1,N
      DF(I)=V(I)
62    AT(I)=XA(I)
46    DO 40 K=1,35
      DO 52 I=1,N
      X1=XX-.01
      X2=XX+.01
      IF (DF(I).LE.X2.AND.DF(I).GE.X1) GO TO 51
      GO TO 52
51    DEVMIN=0.1
      DO 56 I1=1,40
56    DEV(I1)=ABS(DF(I+I1-1)-XX)
      DO 57 I2=1,40
      IF(DEV(I2).GT.DEVMIN) GO TO 57
      DEVMIN=DEV(I2)
      I3=I+I2-1
57    CONTINUE
      A(KK)=AT(I3)
      IF (J.EQ.1)  X(KK)=A(KK)
      IF (J.EQ.2)  Y(KK)=A(KK)
      GO TO 17
52    CONTINUE
      M=KK-1
      IF (J.EQ.1) GO TO 30
      IF (J.EQ.2) GO TO 14
17    KK=KK+1
      XX=XX+.035
40    CONTINUE
30    CONTINUE

14    A1=0.0
      A2=0.0
```

```
      A3=0.0
      A4=0.0
      C1=0.0
      C2=0.0
      C3=0.0
      DO 70 I=1,M
      A1=X(I)+A1
      A2=X(I)**2+A2
      A3=X(I)**3+A3
      A4=X(I)**4+A4
      C1=Y(I)+C1
      C2=X(I)*Y(I)+C2
      C3=X(I)**2*Y(I)+C3
70    CONTINUE
      NUM=M*(C3*(M*A2-A1**2)+C1*(A1*A3-A2**2)-M*A3*C2+A1*A2*C2)
      DEN=M*(A4*(M*A2-A1**2)-M*A3**2+2.*A1*A2*A3-A2**3)
      BETA2=NUM/DEN
      PH=2.*PHD*180./PI
      PRINT 105,PH,BETA2
105   FORMAT(4X,F8.3,6X,E12.6,/)
      BETAT=BETAT+BETA2**2
      WRITE (5,*)BETA2
2     CONTINUE

C   ** ROOT MEAN SQUARE VALUE OF BETA2 **
      BETARMS=SQRT(BETAT/100.)

      PRINT *,BETARMS
      STOP
      END
```

REFERENCES

[1] Hervé Rix and Jean Pierre Malengé, "Detecting small Variations in Shape", IEEE Transactions on Systems, Man, and Cybernetics, Vol. SMC-10, No. 2, February 1980.

[2] Y. Biraud, "A new Approach for Increasing the Resolving Power by Data Processing", Astron. and Astrophysics, Vol. 1, pp. 124-27, 1969.

[3] E. Grushka, "Characterization of Exponentially Modified Gaussian Peaks in Chromatography", Analytical Chemistry, Vol. 44, pp. 1733-1738, 1972.

[4] E. Grushka, M.N. Myers, and J.C. Giddings, "Moments Analysis for the Discernment of Overlapping Chromatographic Peaks", Analytical Chemistry, Vol. 42, pp. 21-26, 1970.

[5] N.L. Johnson and S. Kotz, "Distributions in Statistics: Continuous Univariate Distributions - 1", Boston: Houghton Mifflin, 1970.

[6] J.E. Freund and R.E. Walpole, "Mathematical Statistics", Third Edition, New Jersey: Prentice Hall, 1980.

[7] R.F. Baum, "A Novel Algorithm for Resolution of Point Targets", IEEE Transactions on Aerospace and Electronic Systems, Vol. AES-11, No. 6, November 1975.

[8] G.S. Sandhu and N.F. Audeh, "Measurement of Closely Spaced Point Targets", IEEE Transactions on Aerospace and Electronic Systems, Vol. AES-16, No. 2, March 1980.

[9] G.S. Sandhu, N.F. Audeh, "The Resolution Performance of Range Estimators", IEEE Transactions on Aerospace and Electronic Systems, Vol. AES-17, No. 5, September 1981.

[10] A. Antoniou, "Digital Filters Analysis and Design", New Delhi: Tata McGraw-Hill Publishing Company Ltd., 1980.

[11] A. Papoulis, "Probability, Random Variables and Stochastic Processes", New York: McGraw-Hill, 1965.